**Atmospheric
Chemistry
and Physics
Discussions**

On the roles of sulphuric acid and low-volatility organic vapours in the initial steps of atmospheric new particle formation

P. Paasonen[1], T. Nieminen[1], E. Asmi[2], H. E. Manninen[1], T. Petäjä[1],
C. Plass-Dülmer[3], H. Flentje[3], W. Birmili[4], A. Wiedensohler[4], U. Hõrrak[5],
A. Metzger[6], A. Hamed[7], A. Laaksonen[2,7], M. C. Facchini[8], V.-M. Kerminen[1,2],
and M. Kulmala[1,9]

[1]University of Helsinki, Helsinki, Finland
[2]Finnish Meteorology Institute, Helsinki, Finland
[3]Meteorological Observatory of Hohenpeissenberg, Hohenpeissenberg, Germany
[4]Institute for Tropospheric Research, Leipzig, Germany
[5]University of Tartu, Tartu, Estonia
[6]Ionicon Analytik GmbH, Innsbruck, Austria
[7]University of Eastern Finland, Kuopio, Finland
[8]Institute Atmospheric Sciences and Climate, Bologna, Italy

ACPD

10, 11795–11850, 2010

On the roles of H$_2$SO$_4$ and organic vapours in new particle formation

P. Paasonen et al.

Title Page

Abstract	Introduction
Conclusions	References
Tables	Figures

|◄ | ►|

◄ | ►

Back | Close

Full Screen / Esc

Printer-friendly Version

Interactive Discussion

[9]Stockholm University, Stockholm, Sweden

Correspondence to: P. Paasonen (pauli.paasonen@helsinki.fi)

On the roles of H_2SO_4 and organic vapours in new particle formation

P. Paasonen et al.

Title Page

Abstract	Introduction
Conclusions	References
Tables	Figures

|◄ | ►|

◄ | ►

Back | Close

Full Screen / Esc

Printer-friendly Version

Interactive Discussion

Abstract

Sulphuric acid and organic vapours have been identified as the key components in the ubiquitous secondary new particle formation in the atmosphere. In order to assess their relative contribution and spatial variability, we analyzed altogether 36 new particle formation events observed at four European measurement sites during EUCAARI campaigns in 2007–2009. We tested models of several different nucleation mechanisms coupling the formation rate of neutral particles (J) with the concentration of sulphuric acid ([H$_2$SO$_4$]) or low-volatility organic vapours ([org]) condensing on sub-4 nm particles, or with a combination of both concentrations. Furthermore, we determined the related nucleation coefficients connecting the neutral nucleation rate J with the vapour concentrations in each mechanism. The main goal of the study was to identify the mechanism of new particle formation and subsequent growth that minimizes the difference between the modeled and measured nucleation rates. At three out of four measurement sites – Hyytiälä (Finland), Melpitz (Germany) and San Pietro Capofiume (Italy) – the nucleation rate was closely connected to squared sulphuric acid concentration, whereas in Hohenpeissenberg (Germany) the low-volatility organic vapours were observed to be dominant. However, the nucleation rate at the sulphuric acid dominant sites could not be described with sulphuric acid concentration and a single value of the nucleation coefficient, as K in $J=K$ [H$_2$SO$_4$]^2, but the coefficients seemed to vary between the sites. This inter-site variation was substantially smaller when the heteromolecular homogenous nucleation between H$_2$SO$_4$ and organic vapours was assumed to take place in addition to homogenous nucleation of H$_2$SO$_4$ alone, i.e. $J=K_{SA1}[H_2SO_4]^2+K_{SA2}[H_2SO_4][org]$. By adding in this equation a term describing homomolecular organic vapour nucleation, $K_{s3}[org]^2$, equally good results were achieved. In general, our results suggest that organic vapours do play a role, not only in the condensational growth of the particles, but as well in the nucleation process, with a site specific degree.

Full Screen / Esc

1 Introduction

A large number of observations have shown that atmospheric new particle formation by nucleation takes frequently place in continental boundary layer, as well as in free troposphere (e.g. Kulmala et al., 2004a; Kulmala and Kerminen, 2008; Venzac et al., 2008; Mirme et al., 2010). Under favorable conditions, nucleated particles grow into sizes in which they are able to produce new cloud condensation nuclei (Lihavainen et al., 2003; Kerminen et al., 2005; Laaksonen et al., 2005; Whitehead et al., 2009; Wiedensohler et al., 2009). The important role of nucleation in the global aerosol budget, and thereby in cloud microphysics and climate, has recently been demonstrated by many large-scale modeling studies (Spracklen et al., 2008; Makkonen et al., 2009; Merikanto et al., 2009; Pierce and Adams, 2009; Wang and Penner, 2009; Yu and Luo, 2009).

A successful simulation of aerosol dynamics in global climate or Earth System models requires mechanistic understanding on how the nucleation rate (J) is connected with the concentrations of vapours participating in the nucleation process. At present such an understanding is far from complete. Both field measurements and laboratory experiments have identified sulphuric acid (H$_2$SO$_4$) as the key player in atmospheric nucleation (e.g. Weber et al., 1997; Sipilä et al., 2010). The best relation between the nucleation rate and H$_2$SO$_4$ concentration is usually obtained when assuming $J \sim [\text{H}_2\text{SO}_4]^n$, where the exponent n lies in the range 1–2 (Weber et al., 1997; Kulmala et al., 2006; Riipinen et al., 2007; Kuang et al., 2008; Paasonen et al., 2009; Sipilä et al., 2010). Such a relation is in stark contrast with existing thermodynamic nucleation theories, but it could be explained by activation-type (Kulmala et al., 2006) or kinetic (McMurry and Friedlander, 1979) nucleation involving H$_2$SO$_4$.

In addition to sulphuric acid, the atmospheric nucleation rate has been suggested to be affected by many other trace gases (see Kulmala and Kerminen, 2008). Among them, low-volatile organic compounds are of specific interest for several reasons. First of all, large amounts of organic aerosol precursor vapours are emitted into the global

atmosphere, and in future such emissions might even be increased as a result of climate change (Kulmala et al., 2004b; Arneth et al., 2008; Pacifico et al., 2009; Rinne et al., 2009). Secondly, the contribution of secondary sources to the atmospheric organic aerosol load in general, and to aerosol dynamics in particular, seems to be much larger than previously thought (Hallquist et al., 2009; Jimenez et al., 2009). Thirdly, the growth of freshly-nucleated atmospheric aerosol particles cannot usually be explained without a significant contribution by vapours other than sulphuric acid (Weber et al., 1997; Birmili et al., 2003; Boy et al., 2005; Smith et al., 2008), and indirect chemical measurements indicate that organics are present in nm-sized and larger particles during atmospheric new particle formation events (O'Dowd et al., 2002; Laaksonen et al., 2008). Direct evidence on the participation of organics in the nucleation process has also been obtained in laboratory experiments (Zhang et al., 2004, 2009; Metzger et al., 2010).

The biggest gap of knowledge when linking atmospheric nucleation with organic vapours is the ignorance of the contributing species (e.g. Clayes et al., 2009). As a result, we neither know which organic vapours participate in nucleation, nor their physical and chemical properties, or concentrations. In this paper, we aim to shed new light on the role of organic compounds in atmospheric nucleation. We will approach the problem by first assuming that both nucleation and initial growth of nucleated particles are determined by sulphuric acid and the same low-volatility organic vapour(s). By determining the particle growth rate and gaseous sulphuric acid concentration from measurements, we may calculate the "growth-equivalent" organic vapour concentration and investigate its relation to measured nucleation rates. Besides the simple first and second order mechanism based on sulphuric acid studied before (Kulmala et al., 2006), we will investigate six additional analogous nucleation mechanisms that involve this organic vapour concentration. Our analysis relies on measurements conducted within the EUCAARI project (Kulmala et al., 2009) at four different field sites in central and Northern Europe.

2 Materials and methods

2.1 Measurement sites

The combined data set used in this study was collected from four different stations around Europe (Fig. 1). The sites represent locations with a variable anthropogenic influence and gas phase pollutant levels. The stations also differ significantly in geographical latitude and, consequently, in terms of their surrounding ecosystems – varying from the rural Boreal forest (Hyytiälä) to Mediterranean agricultural areas (San Pietro Capofiume). The altitude range varies from close to sea level in the Po Valley to mountainous Hohenpeissenberg at 985 m.

2.1.1 Hyytiälä

Hyytiälä (SMR) is a rural site in central southern Finland (61°51′ N, 24°17′ E, 181 m a.s.l.). The measurements in Hyytiälä were performed at SMEAR II (Station for Measuring Ecosystem-Atmosphere Relations, operated by University of Helsinki) station (Hari and Kulmala, 2005), which is located in boreal coniferous forest consisting mostly of Scots pine (*Pinus sylvestris* L.). The biggest city nearby Hyytiälä, Tampere, is about 60 km from the site and has a population of about 200 000.

2.1.2 Hohenpeissenberg (HPB)

The Meteorological Observatory Hohenpeissenberg (e.g. Birmili et al., 2003), operated by German Weather Service (DWD), is situated in rural southern Germany (47°48′ N, 11°0′ E), 40 km north from the Alps. The observatory stands on the top of the Hohenpeissenberg Mountain, at an altitude of 985 m a.s.l. and about 300 m above the surrounding countryside. The surroundings of the mountain are mainly meadows and forests.

2.1.3 Melpitz

Melpitz (MPZ; Engler et al., 2007) is a rural site in eastern Germany (51°32′ N, 12°54′ E, 87 m a.s.l.). The measurement site is operated by Leibniz-Institute for Tropospheric Research (IfT), and situated on a flat meadow surrounded by agricultural land. Even though Melpitz is clearly considered a rural observation site, the levels of anthropogenic pollution tend to be higher than in Hyytiälä or Hohenpeissenberg e.g. in terms of sulphur dioxide (Hamed et al., 2010), which is the prime anthropogenic precursor of H_2SO_4.

2.1.4 San Pietro Capofiume (SPC)

San Pietro Capofiume (e.g. Hamed et al., 2007) is located in Northern Italy, in a flat rural area in the eastern part of the Po Valley (44°39′ N, 11°37′ E, 11 m a.s.l.). The distance to the closest cities, Bologna and Ferrara, is about 40 km. Po Valley is the largest industrial, trading and agricultural area in Italy with a high population density. During the measurements reported here, however, fairly clean conditions were encountered with frequent influence of air masses from the Adriatic Sea.

2.2 Instrumentation and measurements

Similar sets of atmospheric particle measurements were carried out during the EUCAARI-campaigns at all four sites: in Hyytiälä from 1 April to 21 May 2007 (Manninen et al., 2009), in Hohenpeissenberg from 20 July 2007 to 28 December 2008, in Melpitz from 10 May to 31 May 2008 (Manninen et al., 2010), and in San Pietro Capofiume from 30 June to 12 July 2009. All four data sets included air ion and neutral particle size distributions, sulphuric acid concentrations and global radiation data.

2.2.1 Ultrafine particle size distributions

The air ion and neutral particle size distributions from 0.8 to 42 nm (mobility diameter) were recorded with Neutral cluster and Air Ion Spectrometers (NAIS; Kulmala et al., 2007; Asmi et al., 2009). The NAIS classifies the particles according to their electrical mobilities, which are further converted to mobility diameters. Ion concentrations are calculated from electrometer currents, both polarities being measured simultaneously with different electrometers. Additionally, the NAIS measures neutral particles by using a corona charged-filter section in front of the mobility analyzer. One measurement cycle, consisting of ion, total (neutral + charged) and background signal measurements, is completed in five minutes. Prior to field measurements, all NAIS instruments were inter-compared and calibrated (Asmi et al., 2009).

2.2.2 Sulphuric acid concentration

The sulphuric acid concentrations were measured with Chemical Ionization Mass Spectrometers (CIMS; Berresheim et al., 2000; Petäjä et al., 2009). The measurements in Hohenpeissenberg, Melpitz and San Pietro Capofiume were performed with the CIMS of DWD, whereas in Hyytiälä the CIMS of the National Center for Atmospheric Research (NCAR, USA) was used.

Measuring sulphuric acid concentration is not a standard procedure hitherto. The sulphuric acid concentration measured with the NCAR CIMS has been compared to calculated concentration proxies in Hyytiälä (Petäjä et al., 2009). The measured concentrations agreed well with those calculated with the proxies. However, intercalibration of different CIMSs has not been performed. Though, we can not fully exclude the possibility of systematic differences in the sulphuric acid concentrations [H_2SO_4] measured by different instruments (NCAR and DWD), both instruments are designed very similar and rely on the same calibration procedure. The uncertainty of the DWD instrument for H_2SO_4 has been estimated to be at 39% (2-sigma) (Berresheim et al., 2000), and has been improved since. Thus, combined uncertainties might result in up to 50%

systematic difference between both instruments in worst case. Systematic differences in sulfuric acid measurements due to instrumental drift between the sites HPB, Melpitz and SPC which were all measured by the same DWD CIMS instrument with identical calibration procedures, should not exceed 20%.

2.2.3 Ancillary data

We utilized for calculations also the particle size distributions from 3 nm up to 800 nm in Melpitz, up to 1 μm in Hyytiälä and up to 600 nm in SPC, all measured with a Differential Mobility Particle Sizer (DMPS; Hoppel, 1978; Aalto et al., 2001; Birmili et al., 1999), and distributions from 13 nm up to 900 nm in HPB measured with a Scanning Mobility Particle Sizer (SMPS).

Additionally, the basic meteorological data (global radiation, temperature, relative humidity, air pressure, and wind speed and direction) were available.

2.3 Data analysis

The goal of this study was to investigate the connections between the formation rate of neutral 2 nm size particles (J_2), and the concentrations of sulphuric acid ([H_2SO_4]) and other vapours condensing on sub 4 nm particles. These vapours were assumed to be oxidized organic vapours and are thus marked with [org] hereafter.

In order to derive J_2 and [org] from the measurements, the particle growth rate (GR) is needed. The growth rate can be determined only if a new growing mode of particles with $d_P \sim 2$ nm is observed and can be distinguished from the size distribution, i.e. on nucleation event days (an example is given in Fig. 2a). Only those nucleation event days, for which a sufficiently unambiguous value for GR could be determined, were used in the analysis. Furthermore, the concentration of particles with diameters from 2 to 4 nm (N_{2-4}) is needed to calculate the J_2. The neutral particle concentration below 3 nm measured with the NAIS can be trusted only when reasonably high concentrations are obtained (Asmi et al., 2009). Thus, to attain reliable GR and N_{2-4} values we

included in the analysis only the data points measured during the nucleation events. The start and the end time of the events were determined visually from the total particle size distributions recorded with the NAIS (see Fig. 2a).

2.3.1 The particle growth rate GR_{2-4}

The growth rate of particles from 2 to 4 nm in diameter (d_P) was determined from the ion size distribution recorded by the NAIS. The ion concentrations were used instead of the total concentrations, because the growing mode is typically better defined in the ion concentrations. The determination of the growth rate was made with the method presented by Hirsikko et al. (2005) as follows. A log-normal mode was fitted to the time series of ion concentrations at every size class with geometric mean diameter from 2 to 4 nm during the nucleation event. A linear fitting to the times corresponding to the maxima of these modes was made, resulting in the growth rate GR_{det} in units $nm\,h^{-1}$ (an example is given in Fig. 2b).

Manninen et al. (2009) assumed that the real growth rate from 2 to 3 nm might be a factor of 2 lower or higher than the average growth rate of particle population determined with the method described above. However, as we used in our analysis only those nucleation events for which the determined growth rate seemed unambiguous, this factor was somewhat smaller.

From the sulphuric acid concentration ([H_2SO_4]) measured with the CIMS we calculated the particle growth rate related to sulphuric acid condensation (GR_{H2SO4}). The sulphuric acid concentration required for growth rate of 1 nm/h in particle size range $d_P = 2–4$ nm was obtained from Nieminen et al. (2010) (see also Lehtinen and Kulmala, 2003)

$$C_{GR=1,\ H2SO4} = \frac{2\,\rho_P d_v}{\gamma m_v \Delta t} \cdot \sqrt{\frac{\pi m_v}{8\,kT}} \cdot \left[\frac{2\,x_1 + 1}{x_1(x_1 + 1)} - \frac{2\,x_0 + 1}{x_0(x_0 + 1)} + 2\ln\left(\frac{x_1(x_0 + 1)}{x_0(x_1 + 1)}\right) \right],\ (1)$$

where x_0 and x_1 are the ratios of the vapour molecule diameter (d_v) to the initial and final particle diameter, respectively. The mass of a sulphuric acid vapour molecule m_v

Full Screen / Esc

Printer-friendly Version

Interactive Discussion

was calculated with the parameterization by Kurtén et al. (2007), describing the sulphuric acid hydrate distribution as a function of ambient temperature (T) and relative humidity. For the density of the particle (ρ_P) we used a value of 1440 kg m^{-3}. This is an average of the density of sulphuric acid-water-mixture (ρ=1670 kg m^{-3}, the average at the conditions of the data points used in the analysis, calculated with the parameterizations by Kurtén et al., 2007, and Jaecker-Voirol, 1988) and the assumed density of the other vapour(s) participating in the nucleation and/or the initial growth of the particles (ρ=1200 kg m^{-3}, see Sect. 2.3.2). Finally, the vapour molecule diameter d_v was calculated separately for each data point as a function of temperature and humidity, by using the mass m_v and the density of the sulphuric acid-water-mixture.

Actually, the calculated $C_{GR=1,H2SO4}$ describes the theoretical minimum H$_2$SO$_4$ concentration leading to a growth rate of 1 nm h^{-1}, as it is assumed that every sulphuric acid molecule colliding with the particle is attached to it. However, in laboratory experiments by Sipilä et al. (2010) the observed growth was in good agreement with the growth calculated with Eq. (1). This gives us confidence on the assumption of collision limited growth rate. For further details concerning the derivation of Eq. (1), we refer the reader to Nieminen et al. (2010).

The growth rate related to H$_2$SO$_4$ condensation during the timeframe used for the determination of GR$_{det}$ was calculated directly as

$$GR_{H2SO4} = \frac{[H_2SO_4]_{det}}{C_{GR=1,\ H2SO4}}. \tag{2}$$

For the sulphuric acid concentration [H$_2$SO$_4$]$_{det}$ we used the one hour median of the measured concentrations recorded during the corresponding timeframe for determination of GR$_{det}$.

2.3.2 Estimated concentration of the low-volatility organic vapours

The identity of vapours other than sulphuric acid influencing the new particle formation is not known hitherto. Therefore we had to estimate their properties and concentration

indirectly. We assumed that the vapours potentially participating in nucleation are the same as those causing the part of the condensational growth of the smallest freshly nucleated particles (d_P=2–4 nm), which can not be explained by sulphuric acid. Although no clear evidence of the composition of these vapours is available, we assumed that they are of organic origin (e.g. Kulmala et al., 2004b; Riipinen et al., 2009). The growth rate related to condensation of these vapours was calculated from the previously described growth rates as the difference between the observed growth rate and that due to sulphuric acid condensation, i.e.

$$GR_{org} = GR_{det} - GR_{H2SO4}, \tag{3}$$

where GR_{det} refers to the observed growth rate.

We approximated the properties of the organic vapour species with those of monoterpene oxidation products, with the chemical formula $C_{10}H_{16}O_2$ (Taipale et al., 2008). The corresponding molecule mass is 168 amu, and for the density we assumed a value of 1200 kg m^{-3}. With these estimations, using Eq. (1), we calculated the organic vapour concentration $C_{GR=1, \, org}$ leading to 1 nm h^{-1} growth, and further the organic vapour concentration needed to produce GR_{org} as

$$[org]_{det} = GR_{org}C_{GR=1, \, org}. \tag{4}$$

As stated earlier, Eq. (1) gives the theoretical minimum of the vapour concentration needed for the 1 nm h^{-1} growth. Thus, the concentration calculated in Eq. (4) is the minimum concentration of low-volatility organic vapours needed for completing the observed growth rate.

With the above described method we could derive one value per day for the growth rate of the particles and thereby also for the concentration of condensing oxidized organic vapours. However, the concentration of oxidized organic vapours is expected to vary significantly during the day, due to the variation in both their source, the oxidation rate of precursor vapours, and sink, condensation to ambient aerosol. Because the concentration of the precursor vapours could not be determined, we approximated the

concentration of the oxidized organic vapours to be directly proportional to the concentration of hydroxyl radical (OH), and inversely proportional to the condensational sink CS (Kulmala et al., 2001). The oxidized organic vapours condensing on the sub 4 nm particles were assumed to be produced via OH oxidation neglecting the other important day time oxidation pathway, ozonolysis (Hao et al., 2009; Kulmala et al., 2004b). Even if this assumption did not hold exactly, the ozone concentration does not have as strong a diurnal variation as the OH concentration and thus would not have as drastic impacts on the diurnal cycle of [org] as does the hydroxyl radical concentration. Since the measured OH concentration was not available from all the measurement sites, we approximated the diurnal variation of OH concentration by the variation observed in global radiation. This is justified, since the main atmospheric pathway in the production of OH-radical is the photolysis of ozone by UV-B light (Rohrer and Berresheim, 2006), which at the same time correlates well with the global radiation. Hence, the estimated concentration of the oxidized organic vapours is written as

$$[\text{org}] = [\text{org}](t) = [\text{org}]_{\text{det}} \frac{\text{GlobRad}(t)/\text{GlobRad}_{\text{det}}}{\text{CS}(t)/\text{CS}_{\text{det}}}, \tag{5}$$

where CS refers to the condensational sink for organic vapours, calculated from the DMPS/SMPS data by using the dry size of the particles. The indices "det" refer to the one hour median values during the timeframe of determination of the growth rate. Using this scaled organic vapour concentration we calculated the time dependent growth rate of the particles

$$\text{GR}_{2-4} = \frac{[\text{H}_2\text{SO}_4]}{C_{\text{GR}=1, \text{H2SO4}}} + \frac{[\text{org}]}{C_{\text{GR}=1, \text{org}}}. \tag{6}$$

2.3.3 Particle formation rate J_2

When measuring on the total particle mode of the NAIS, not only the neutral particles are counted, but also the natural external ions of the same size. Typically the NAIS

11807

detects high total concentrations of particles below 2 nm size (e.g. Fig. 2a). A fraction of these particles can be real atmospheric clusters (Kulmala et al., 2007) which, however, can not be readily distinguished from the ions produced in the corona charger of the instrument (Asmi et al., 2009). Due to this uncertainty, the total particle concentrations were only calculated down to 2 nm diameter limit. However, this diameter is adequate, because the diameter of the stable particles formed in nucleation is assumed to be between 1 and 2 nm (e.g. Kulmala et al., 2007; Nieminen et al., 2009; Sipilä et al., 2010).

The particle formation rate (J_2^{tot}, where index 2 refers to the formation of particles with d_P=2 nm, and "tot" to total as both neutral and charged) was calculated with the method presented by Riipinen et al. (2007) and Kulmala et al. (2007), by using the concentration N_{2-4}^{tot} of 2 to 4 nm particles measured with the NAIS, and the time derivative dN_{2-4}^{tot}/dt of this concentration in the equation

$$J_2^{tot} = \frac{dN_{2-4}^{tot}}{dt} + \frac{GR_{2-4}N_{2-4}^{tot}}{4\,nm - 2\,nm} + CoagS_3 N_{2-4}^{tot}, \tag{7}$$

where $CoagS_3$ is the coagulational sink (Kulmala et al., 2001) for particles with d_P=3 nm (close to the geometric mean of the size bin 2–4 nm), calculated from the DMPS/SMPS data. On the right hand side of Eq. (7), the first term represents the observed change of the concentration, the second term is the growth out of the specified size range and the third term describes the coagulational scavenging. In calculation of $CoagS_3$, we used the dry size of the particles.

2.3.4 Charged and neutral particle formation rates

The formation rates of positively and negatively charged particles with diameter d_P=2 nm (J_2^+ and J_2^-, respectively) were calculated from the ion size distributions measured with the NAIS almost similarly as the total particle formation rate J_2^{tot}. However, two additional terms appear in the equation: a sink of ions with d_P=2–4 nm caused

by their recombination with the ions of the opposite polarity, and a source due to the charging of neutral particles via coagulation with smaller ions. Thus, the formation rate of positively charged particles may be written as (Manninen et al., 2009)

$$J_2^+ = \frac{dN_{2-4}^+}{dt} + \frac{GR_{2-4}N_{2-4}^+}{4\,nm - 2\,nm} + CoagS_3 N_{2-4}^+ + \alpha \cdot N_{2-4}^+ N_{<4}^- - \beta \cdot N_{2-4}^{tot} N_{<2}^+. \qquad (8)$$

5 The formation rate of negatively charged particles J_2^- is calculated equally but using the opposite polarities. In Eq. (8) $N_{<d}$ denotes the concentration of ions with diameter smaller than d nm, $\alpha = 1.6 \times 10^{-6}$ cm^3 s^{-1} is the recombination coefficient (Israël, 1970), and $\beta = 1.0 \times 10^{-8}$ cm^3 s^{-1} is the ion-neutral particle attachment coefficient (Tammet and Kulmala, 2005).

10 In order to examine the neutral fraction of J_2^{tot}, we subtracted the ion formation rates, and achieved

$$J_2 = J_2^{tot} - J_2^+ - J_2^-. \qquad (9)$$

We also calculated the recombination rate (J_{rec}) producing neutral particles with 2–4 nm size. This was done by summing the products of the concentrations of those
15 opposite polarity ions that would colliding with each other produce a particle with $d_P = 2$–4 nm, and multiplying this sum with the recombination coefficient α. This method is more precisely described by Manninen et al. (2009). The recombination coefficient α describes the collision rate of opposite polarity ions, and is thus the maximum rate coefficient for production of stable neutral particles via recombination. There is no
20 evidence and thus no reason to believe that the recombination product would still be stable, when the electrical forces holding each of the charged particles together are vanished. Because we do not thereby know how large fraction of the recombined ion pairs affects our measured J_2, we did not subtract J_{rec} in calculation of the neutral particle formation rate J_2. Instead, the values of J_{rec} were used in order to investigate
25 which fraction of J_2 could be explained by the recombination of ions.

The particle formation rate data were filtered with a parabolic differentiation algorithm (with a window size of 3 data points, i.e. 30 min), in order to reduce the fluctuations in

J_2 data resulting from the noise in the calculation of the derivative dN_{2-4}/dt. Finally, the particle formation rate data was interpolated to the 10 min time steps of the sulphuric acid concentration data.

2.3.5 On the uncertainties of N_{2-4} measured with the NAIS

We do accept the inaccuracy of the NAIS, when measuring the concentrations $N_{<3}$ of neutral particles with diameters below 3 nm (Asmi et al., 2009). This inaccuracy arises mainly from the charger ions, some fraction of which is detected as neutral particles with diameters below 3 nm. However, as Asmi et al. (2009) state, this relative inaccuracy decreases, when the ambient $N_{<3}$ is high, which is the case in all our analyzed data points measured during the nucleation events. If the charger ions did affect the observed N_{2-4}, their effect on J_2^{tot} would be most significant, when both actual N_{2-4} and its time derivative are relatively small i.e. in the data points with the smallest J_2^{tot} (see Eq. 7). This effect would cause slight overestimation of J_2^{tot} in these data points.

2.4 The studied nucleation mechanisms

We investigated the models of two existing nucleation theories, activation and kinetic theories, and six more or less new suggestions for neutral nucleation mechanisms. According to the activation theory, the sulphuric acid molecules activate the pre-existing neutral clusters with $d_P<2$ nm to further growth (Kulmala et al., 2006). Thereby, the number of activated clusters (i.e. formed particles) is linearly connected to the sulphuric acid concentration

$$J = A\,[H_2SO_4],\tag{10}$$

where A is the activation coefficient.

Kinetic theory (McMurry and Friedlander, 1979) assumes homogenous homomolecular nucleation to occur between two sulphuric acid molecules as in gas kinetic theory, and thus the nucleation rate is connected to the squared sulphuric acid concentration

$$J = K\ [H_2SO_4]^2.\tag{11}$$

Here the kinetic coefficient K is not only the reaction rate coefficient, but includes both the collision frequency and the probability of formation of a stable particle after the collision (Weber et al., 1997; Sihto et al., 2006).

The activation and kinetic theories suggest that the nucleation rate is proportional to sulphuric acid concentration alone. The following mechanisms were derived assuming that the organic vapours participating in the initial growth of the nucleated particles are involved in the nucleation process itself, as well. The first studied mechanisms are equal to activation and kinetic theory, but the organic species is supposed to induce the nucleation instead of the sulphuric acid, either via cluster activation

$$J = A_{org}\ [org],\tag{12}$$

or by homogenous nucleation

$$J = K_{org}\ [org]^2,\tag{13}$$

in which [org] stands for the concentration of the oxidized organic vapours condensing on sub 4-nm particles.

If we assume that both sulphuric acid and organic vapour can activate the pre-existing unidentified clusters, we can write

$$J = A_s\ ([H_2SO_4] + [org]).\tag{14}$$

The next proposed mechanism presumes either homogenous heteromolecular nucleation between sulphuric acid and organic vapour molecules, or one of the vapours activating the clusters composed around a molecule of the other vapour, resulting in

$$J = K_{het}\ [H_2SO_4][org].\tag{15}$$

On the roles of H₂SO₄ and organic vapours in new particle formation

P. Paasonen et al.

Title Page

Abstract | Introduction

Conclusions | References

Tables | Figures

◄ | ►

◄ | ►

Back | Close

Full Screen / Esc

Printer-friendly Version

Interactive Discussion

If in addition to heteromolecular nucleation (Eq. 15) the homogenous homomolecular nucleation of sulphuric acid takes place, we have

$$J = K_{SA} ([H_2SO_4]^2 + [H_2SO_4][org]), \tag{16}$$

and if also the organic vapours can nucleate homomolecularly

$$J = K_s ([H_2SO_4]^2 + [H_2SO_4][org] + [org]^2). \tag{17}$$

In order to make it easier for the reader to understand the previously introduced coefficients with several subscript indices, some clarification for the choice of the indices follows: all the coefficients A refer to activation of pre-existing clusters while coefficients K refer to homogenous (kinetic type) nucleation; coefficients with no indices refer to the previously presented theories taking into account only the sulphuric acid concentration, index "org" refers to activation/nucleation by organic vapours solely, "s" to the sum of vapours or vapour combinations, "het" is connected with heteromolecular homogenous nucleation, and "SA" with the homogenous nucleation of sulphuric acid with both of the available vapours.

The activation and kinetic theories (Eqs. 10–11) have been studied in several articles, such as Kulmala et al. (2006), Sihto et al. (2006), Riipinen et al. (2007) and Paasonen et al. (2009). Also the heteromolecular homogenous nucleation mechanism (Eq. 15) has been investigated in laboratory conditions by Metzger et al. (2010). The rest of the above presented mechanisms are to our best knowledge studied here for the first time.

2.4.1 Optimized separate nucleation coefficients

In addition to the above described nucleation mechanisms (Eqs. 10–17), we studied those mechanisms in which more than one term exist (Eqs. 14, 16 and 17) with separated coefficients for each term. By introducing these separate nucleation coefficients, the Eqs. (14), (16) and (17) are written as

$$J = A_{s1} [H_2SO_4] + A_{s2} [org], \tag{18}$$

$$J = K_{\text{SA1}} [\text{H}_2\text{SO}_4]^2 + K_{\text{SA2}} [\text{H}_2\text{SO}_4] [\text{org}] \tag{19}$$

and

$$J = K_{\text{s1}} [\text{H}_2\text{SO}_4]^2 + K_{\text{s2}} [\text{H}_2\text{SO}_4] [\text{org}] + K_{\text{s3}} [\text{org}]^2. \tag{20}$$

The evaluation of the above coefficients was made by minimizing the sum of the squares of the difference between observed and modeled nucleation rate in every data point.

Different coefficients for separate terms can be expected, because the chemical properties of the sulphuric acid molecule and low-volatility organic vapour molecules are expected to be different, which will lead to varying concentrations needed to achieve a given activation and homogenous nucleation rates. Actually, among the condensing organic vapour molecules, there may be several vapours with different chemical composition and physical properties, but in this study we have no way to do more than treat these organic vapours as a bulk.

2.4.2 Comparison of the nucleation mechanism models

The comparison between the models of the different nucleation mechanisms was done both for the whole data set and site by site. Our comparison is based on the following criteria :

 – the correlation coefficient R between the logarithms of the observed (Eq. 9) and modeled neutral nucleation rate.

 – The variation $V_{90/10}$, i.e. the ratio of 90th and 10th percentiles of the data point-specific ratio between the observed and modeled nucleation rate. For example, when determining the $V_{90/10}$ for the H$_2$SO$_4$ activation mechanism $J = A[\text{H}_2\text{SO}_4]$, we first calculate the ratio $J_2/[\text{H}_2\text{SO}_4]$ in every data point, and then the 90th and 10th percentiles of these ratios. The variation $V_{90/10}$ is simply the ratio of these

percentiles. If the resulting variation was $V_{90/10}=10$, then 80% of the data point-specific coefficients $A(=J_2/[\text{H}_2\text{SO}_4])$ would be within one order of magnitude. Similarly, $V_{90/10}=100$ would mean two orders of magnitude difference between the 90th and 10th percentiles.

5 – The dependency between the logarithms of the observed and modeled nucleation rate, in order to approximate the slope connecting these logarithms. If the slope significantly differs from one, the physical reasoning behind the modeled mechanism does not hold. This is because the slope in logarithmic scale equals to the exponent in linear scale, and, for example, a slope of 0.5 in figure $\log(J_2)$
10 vs. $\log([\text{H}_2\text{SO}_4][\text{org}])$ would mean a connection $J_2 \sim ([\text{H}_2\text{SO}_4][\text{org}])^{0.5}$, which does not follow from the derivation of Eq. (15). The slope was estimated visually instead of linear fitting, because the commonly used linear least squares fitting should not be used when the relative error in both x- and y-directions is significant, and e.g. the bivariate fitting method presented by York et al. (2004) could not be used
15 due to the lack of proper error estimates for each quantity.

Some notes must be made on these comparison methods. First of all, as the correlation coefficients R are calculated for logarithmic values, the exponent of the vapour concentration does not have an effect on R, i.e. equal R results for $J_2 \sim [\text{H}_2\text{SO}_4]$ and $J_2 \sim [\text{H}_2\text{SO}_4]^2$. On the contrary, the variation $V_{90/10}$ is sensible on the order of the gas
20 concentration, not only giving smaller values when the exponent is correct, but also systematically giving larger values for the mechanisms involving second order vapour concentrations (exponent 2 and/or term $[\text{H}_2\text{SO}_4][\text{org}]$). This is logical, because the relative error $\Delta f/f$ e.g. for $f=[\text{H}_2\text{SO}_4]^2$ is twice as large as that for $f=[\text{H}_2\text{SO}_4]$, as can be realized with simple calculations concerning the propagation of error. Furthermore,
25 the larger inaccuracy of [org] compared to $[\text{H}_2\text{SO}_4]$ increases the $V_{90/10}$ values for the organic vapour related mechanisms. Thus, even though the values of R and $V_{90/10}$ give us understanding on the reliability of the different modeled nucleation mechanisms, the visual examination is crucial for determining the reasonability of the models.

3 Results and discussion

3.1 Site specific vapour concentrations, growth and particle formation rates

The concentration $C_{\text{GR=1, H2SO4}}$ needed for $1\,\text{nm}\,\text{h}^{-1}$ growth varied between 7.4×10^6 and $8.8\times10^6\,\text{cm}^{-3}$ due to the differences in ambient temperature and relative humidity. The fraction of growth rate related to sulphuric acid condensation from particle growth rate GR_{det} was, as expected, clearly dependent on the sulphuric acid concentration (Fig. 3).

For the organic vapour, we did not have hydrate distribution or density parameterizations available, and thus, using the oxidized monoterpene properties presented in Sect. 2.3.2 we determined a constant minimum concentration $C_{\text{GR=1, org}}{=}6.5\times10^6\,\text{cm}^{-3}$ that would be required to produce a growth rate of $1\,\text{nm}\,\text{h}^{-1}$ due to the organic vapour condensation.

The median values of the observed growth rate, sulphuric acid concentration, calculated low-volatility organic vapour concentration, and neutral and charged particle formation rates for each measurement site are presented in Table 1. It should be kept in mind that the presented median values in Hohenpeissenberg are calculated for nucleation events which were measured all around the year, whereas at the other sites the measurements were carried out during the late spring or summer months only. Unfortunately, during these months (April–July) only two analyzable nucleation events were recorded at Hohenpeissenberg (partly due to the use of DWD CIMS at the other measurement sites) and thus a detailed spring/summer comparison could not be carried out.

The median sulphuric acid concentration was approximately an order of magnitude higher in Melpitz and SPC ($[\text{H}_2\text{SO}_4]{\sim}10^7\,\text{cm}^{-3}$) than in Hyytiälä and HPB ($[\text{H}_2\text{SO}_4]{\sim}10^6\,\text{cm}^{-3}$), whereas the estimated organic vapour concentration was higher in HPB and SPC ($[\text{org}]{>}3\times10^7\,\text{cm}^{-3}$) than in Hyytiälä and Melpitz ($[\text{org}]{\sim}10^7\,\text{cm}^{-3}$). In Hyytiälä and Hohenpeissenberg, the sulphuric acid induced fraction from the total

On the roles of H$_2$SO$_4$ and organic vapours in new particle formation

P. Paasonen et al.

Title Page

Abstract	Introduction
Conclusions	References
Tables	Figures

|◄ | ►|
◄ | ►

Back | Close

Full Screen / Esc

Printer-friendly Version

Interactive Discussion

growth did not exceed 15%, whereas in Melpitz and SPC the sulphuric acid concentration could explain from 15 to 72% of the observed growth.

The median neutral particle formation rates J_2 were about five times higher in SPC and Melpitz than in Hohenpeissenberg and Hyytiälä (13, 9.4, 2.3 and $1.9\,\mathrm{m^{-3}\,s^{-1}}$, re-
5 spectively). In the whole data set, J_2 varied between 0.01 and $80\,\mathrm{m^{-3}\,s^{-1}}$.

We also calculated the maximum recombination rate J_{rec} producing particles with diameters from 2 to 4 nm. The median ratio J_{rec}/J_2 was 0.015. This ratio exceeded 0.1 in 9% of the data points, and only in 4% of the data points it exceeded 0.2. Thus, the recombination of ions does not explain such a large part of the neutral particle forma-
10 tion rate, that the studied connection between J_2 and vapour concentrations would be drastically affected with it.

3.2 The couplings between J_2 and the vapour concentrations

The correlation coefficients R between the logarithms of the observed and modeled neutral particle formation rates J_2 are presented in Table 2, as well as the variations
15 $V_{90/10}$ i.e. the ratios of 90th and 10th percentile values of the ratios between observed and modeled nucleation rate in each data point. Also the correlation and variation achieved with a linear coupling between J_2 and GR is presented for comparison (see Sect. 3.3.3).

3.2.1 Sulphuric acid nucleation

20 The correlation between neutral particle formation rate J_2 and sulphuric acid concentration [H_2SO_4] was quite strong in Hyytiälä, Melpitz and SPC (correlation coefficients R of 0.58, 0.69 and 0.59, respectively), and when the data of all the sites were considered (R=0.66). However, in Hohenpeissenberg the correlation between J_2 and [H_2SO_4] was weak (R=0.17). J_2 as a function of [H_2SO_4] is presented for all the measurement
25 places in Fig. 4. The 90th and 10th percentile values for coefficient A are shown in the figure, as well.

In Fig. 4 all the data points are quite well located in the same range of coefficients A. However, the data points of the individual sites seem to request slope larger than one (slope one equals to the slope of the percentile lines in figures). This is illustrated more clearly in Fig. 5, where the formation rate at every site is presented separately as a function of squared sulphuric acid concentration. In Fig. 5 the data recorded at HPB between April and July are marked separately. Even though these data points are from only two nucleation event days, they suggest that in HPB the nucleation rate is not well described with models based on sulphuric acid alone even during the spring and summer months.

Even though Fig. 5 clearly shows that J_2 is connected to $[H_2SO_4]^2$ in Hyytiälä, Melpitz and SPC, the values for coefficients K are from one to two orders of magnitude higher in Hyytiälä and HPB than in Melpitz and SPC. This leads to a large variation, $V_{90/10}=180$, for the entire data set (see Table 2). Also the $V_{90/10}$ values for the individual sites are higher than those resulting from the activation mechanism. However, this does not necessarily mean that the activation mechanism would be closer to reality, as mentioned in Sect. 2.4.2. The correlations and variations are discussed in more details in Sect. 3.3.

3.2.2 Organic vapour nucleation

In Hohenpeissenberg the neutral new particle formation rate J_2 correlates well, instead of $[H_2SO_4]^2$, with the low-volatility organic vapour concentration $[org]^2$, $R=0.61$ (Fig. 6). In Hyytiälä this correlation is clearly weaker ($R=0.29$) and it is non-existing or even negative in SPC and Melpitz.

3.2.3 Nucleation of both sulphuric acid and organic vapour

The correlation coefficients between J_2 and the studied combinations of $[H_2SO_4]$ and $[org]$ including homogenous heteromolecular nucleation (term $[H_2SO_4][org]$) but not homogenous organic vapour nucleation (Eqs. 15 and 16) were fairly strong ($R=0.61$

and 0.68, respectively) for the entire data set (see Table 2). The heteromolecular kinetic nucleation (Eq. 15) lead to the smallest variation ($V_{90/10}$=32) amongst the mechanisms related to second order gas concentration and a single nucleation coefficient, when all the data was considered. However, the best correlation coefficient, R=0.68, for the models using single nucleation coefficient was achieved with Eq. (16) (Fig. 7), suggesting both homogenous heteromolecular and homogenous homomolecular nucleation of sulphuric acid to take place. This model also results in smaller site-specific $V_{90/10}$ values for Hyytiälä, Melpitz and SPC than the model of the heteromolecular nucleation alone (Eq. 15) does. Regardless the good correlation, the slope for the whole data set in Fig. 7 seems to be smaller than one.

3.2.4 The optimized nucleation coefficients

The presented optimized nucleation coefficients (Table 3), and the variations and correlation coefficients (Table 2) resulting from their insertion into Eqs. (18) to (20) were obtained by minimizing the sum of squares of the differences in observed and modeled new particle formation rate. Only the parameters optimized for the whole data set, all measurement sites together, are presented here.

The modeled mechanism connecting J linearly with the sum of the vapour concentrations (Eqs. 14 and 18) resulted in remarkably larger correlation coefficient and smaller variation with separated coefficients A_{s1} and A_{s2} than with A_s alone (Table 2). With this model, by using values A_{s1}=7.3×10^{-7} and A_{s2}=6.1×10^{-8} s^{-1}, the highest correlation coefficient and smallest variation (R=0.78, $V_{90/10}$=8) for the whole data set were achieved. However, even with these coefficients, the site-specific data sets seem to be better described with slope values over one (Fig. 8).

The optimization of the separated nucleation coefficients in Eq. (19), modeling homogenous nucleation of sulphuric acid both homomolecularly and heteromolecularly, resulted in values K_{SA1}=8.2×10^{-15} and K_{SA2}=7.0×10^{-14} cm^3 s^{-1}. These coefficients lead to higher correlation coefficient and smaller variation (R=0.73, and $V_{90/10}$=27), compared to those achieved with single nucleation coefficient (Eq. 16) (R=0.68, and

$V_{90/10}$=33). The introduction of a term describing the homogenous homomolecular nucleation of the organic vapours (Eq. 20 with K_{s1}=9.2×10^{-15}, K_{s2}=5.8×10^{-14} and K_{s3}=9.8×10^{-16} cm^3 s^{-1}) had only minor influence on the correlation and variation resulting from Eq. (19). Also the figures depicted for Eq. (19) (Fig. 9) and Eq. (20) (figure not shown) were very similar. Nevertheless, both of these models brought the data from the different sites closer to overall slope one than Eq. (16), as can be seen by comparing Figs. 7 and 9. Furthermore, compared to Fig. 8 presenting J_2 vs. the sum of the first order gas concentrations, the data points of the individual sites agree much better with the slope one in Fig. 9.

3.2.5 Values of the derived nucleation coefficients

The mean, median and percentile values (10th, 25th, 75th and 90th) of the nucleation coefficients for the whole data set, as well as the site specific medians, are presented in Table 4. We would like to emphasize, that these values should be considered as estimative, mostly due to the uncertainties in the determination of the growth rate. Thus, the uncertainties are noticeable especially in the models including organic vapour concentration, calculated using the growth rate, but as order of magnitude estimates they should be reliable.

It is remarkable, that in Table 4 all the median nucleation coefficients related to the models describing kinetic nucleation mechanisms are smaller in SPC than in Hyytiälä or Melpitz. The difference in the median value of K between Hyytiälä (K=1.4×10^{-12} cm^3 s^{-1}) and Melpitz or SPC (K~3×10^{-14} cm^3 s^{-1}) cannot be explained with the possible systematic error arisen from the use of different CIMSs. If we assume that the NCAR CIMS used in Hyytiälä shows 50% lower concentrations than the DWD CIMS (see Sect. 2.2.2), and thus multiply [H$_2$SO$_4$] measured in Hyytiälä with factor 2, the median value of K in Hyytiälä decreases to 3.6×10^{-13} cm^3 s^{-1}. This value is still an order of magnitude higher than the medians of K in SPC and Melpitz.

Title Page

Abstract | Introduction

Conclusions | References

Tables | Figures

|◄ | ►|

◄ | ►

Back | Close

Full Screen / Esc

Printer-friendly Version

Interactive Discussion

3.3 Discussion

3.3.1 The connections between J_2 and first order gas concentrations

In Hyytiälä, Melpitz and SPC the neutral nucleation rate J_2 was closely connected to sulphuric acid concentration ($[H_2SO_2]$), the correlation coefficients R for the logarithms of these quantities were 0.58, 0.69 and 0.59, respectively. However, in Hohenpeissenberg J_2 was clearly better coupled with the calculated concentration of low-volatility organic vapours ($[org]$), $R=0.61$, than with the sulphuric acid concentration ($R=0.17$). The equally high correlation coefficient between J_2 and $[org]$ in Hohenpeissenberg, than between J_2 and $[H_2SO_2]$ at the other sites was quite remarkable, because the organic vapour concentration calculated using $[H_2SO_2]$ and growth rate involves definitely larger uncertainties than those connected to measured sulphuric acid concentration.

When the sum of the gas concentrations ($[H_2SO_4]+[org]$) was investigated instead of $[org]$ solely, the correlation in HPB, $R=0.61$, was equal to that of J_2 and $[org]$. This could be expected, since in HPB the calculated organic vapour concentration was almost an order of magnitude higher than sulphuric acid concentration. At all the other measurement sites the connection between J_2 and the sum is clearly weaker than between J_2 and sulphuric acid alone.

The highest correlation coefficient and smallest variation for the entire data set, $R=0.78$ and $V_{90/10}=8$, were achieved with the model involving the sum of the vapour concentrations with separate sulphuric acid and organic activation coefficients $A_{s1}=7.3\times10^{-7}\,\mathrm{s^{-1}}$ and $A_{s2}=6.1\times10^{-8}\,\mathrm{s^{-1}}$ (Eq. 18). For Hyytiälä, Melpitz and SPC individually these nucleation coefficients produced practically equal correlation and variation than pure sulphuric acid activation. In HPB, the above mentioned separate activation coefficients resulted in weaker correlation and a bit larger variation than with organic vapour concentration alone or with one coefficient A_S multiplying the sum of concentrations. Nevertheless, in all the models for activation type nucleation mechanisms the site-specific data sets seemed to demand slopes steeper than one (Figs. 4 and 8), and thus these models did not describe the nucleation rate reliably.

3.3.2 The connections between J_2 and second order vapour concentrations

The models related to the homogenous nucleation of one of the vapours solely (Eqs. 11 and 13) led to large variations of the coefficient K or K_{org} when all the data is examined together ($V_{90/10}$=180 and 187, respectively). However, by analyzing the variations of the data from the individual sites, we observed that in Hyytiälä the variation of the coefficient K was about twice as large as the variation of coefficient A, and in Melpitz and SPC the difference was even smaller. In HPB the variation of K_{org} was also approximately twice as large as that of A_{org}. As discussed in Sect. 2.4.2, these differences of variations between the models using first and second order vapour concentrations can be expected to result from the propagating uncertainty when the vapour concentration is squared. Visual estimation of the slopes for the separate sites from the figures J_2 vs. [vapour]^n resulted in favor of n=2 (Figs. 5 and 6), as well.

The site-specific median values for coefficient K varied by almost two orders of magnitude, from $K \sim 3 \times 10^{-14}$ cm^3 s^{-1} in Melpitz and SPC to $K = 1.4 \times 10^{-12}$ cm^3 s^{-1} in Hyytiälä (Table 4). Kuang et al. (2008) have reported kinetic coefficient values related to varying continental air mass types in range 1.6×10^{-14}–1.6×10^{-11} cm^3 s^{-1}, with which our results agreed well. Their best fit value for the kinetic coefficient during two nucleation events in March 2003 in Hyytiälä was 4.0×10^{-13} cm^3 s^{-1}, with 90% confidence intervals from 1.3×10^{-13} to 1.2×10^{-12} cm^3 s^{-1}.

Combining the rather small site-specific $V_{90/10}$ values for coefficient K with the remarkable difference in the site-specific medians, we may suggest some interpretations for this: (i) if the homogenous sulphuric acid nucleation is the only nucleation mechanism (in the other stations than HPB), the coefficient K must be dependent of some quantity, which differs significantly between Hyytiälä and Melpitz/SPC, or (ii) there is some other nucleation mechanism in addition to the homogenous H_2SO_4 nucleation taking place especially in Hyytiälä.

The model of homogenous heteromolecular nucleation mechanism proposing the connection $J = K_{het}[H_2SO_4][org]$ resulted in strong correlation for the whole data set

($R=0.61$), and quite strong correlation in Hyytiälä, Hohenpeissenberg and SPC separately (0.51, 0.47 and 0.47, respectively). On the other hand, in Melpitz, where the sulphuric acid concentration was higher than organic vapour concentration, the correlation was clearly weaker ($R=0.30$) than for the mechanisms connecting J with sulphuric
5 acid concentration solely.

When both heteromolecular and homomolecular H_2SO_4 nucleation were assumed to take place, i.e. $J=K_{SA}$ ($[H_2SO_4]^2+[H_2SO_4][org]$), the strongest correlation ($R=0.68$) for the models with a single nucleation coefficient was achieved. Additionally, the variations for the individual sites were smaller than those of any other modeled mechanism
10 connected to second order vapour concentrations, except for HPB where the variation is the smallest for $J=K_{org}[org]^2$. However, the estimated slope connecting the logarithms of modeled and observed particle formation rate from the whole data set does not seem to be one. This can be seen in Fig. 7 as the data points of Melpitz and SPC data sets should be moved either up or left in order to achieve the overall slope one.
15 Introducing the separate nucleation coefficients K_{SA1} and K_{SA2} (Eq. 19) and adding a term of homogenous homomolecular organic vapour nucleation (Eq. 20) lead to higher correlation coefficients and smaller variations ($R=0.73$ and 0.72, and $V_{90/10}=27$ and 26, respectively) than those achieved with single nucleation coefficient K_{SA} ($R=0.68$, $V_{90/10}=33$). The separate coefficients in Eq. (19) with values $K_{SA1}=8.2\times10^{-15}$ cm^3 s^{-1}
20 and $K_{SA2}=7.0\times10^{-14}$ cm^3 s^{-1} and in Eq. (20) with $K_{s1}=9.2\times10^{-15}$, $K_{s2}=5.8\times10^{-14}$ and $K_{s3}=9.8\times10^{-16}$ cm^3 s^{-1} brought especially the Melpitz data points closer to the same slope one with the Hyytiälä and HPB data (Fig. 9). On the other hand, even with these coefficients the modeled formation rate in SPC remains higher than the observed J_2.

3.3.3 On the correlation between J_2 and GR$_{2-4}$

25 Correlation between J_2 and the growth rate of the particles from 2 to 4 nm was significant ($R>0.49$) when calculated for the whole data set from four sites, and for HPB and Melpitz measurement stations alone (Table 2). Thus, one could suspect that the GR

On the roles of H_2SO_4 and organic vapours in new particle formation

P. Paasonen et al.

dependence of J_2^{tot} (Eq. 7) is the reason for the correlations between J_2 and the modeled nucleation mechanisms involving [org] derived from GR (Eqs. 3 and 4). This suspicion is justified, since the GR-term in Eq. (7) covers over 50% of the total J_2^{tot} in some data points. On the other hand, the correlation is inevitable, because the same vapours are expected to take part in both the formation and initial growth of the particles. The most convincing modeled mechanisms (Eqs. 16, 19 and 20) resulted in stronger correlations between the observed and modeled nucleation rates in all measurement sites except HPB (and Melpitz in case of Eq. 19) than the correlations between J_2 and GR. This implies that the correlations are not only due to GR dependence of J_2.

The other reason to be suspicious with the use of GR is that the diameter of 2 nm might be larger than the diameter of the critical stable cluster. Thus, the formation rate of 2 nm particles can be dependent on the growth rate also due to physical reasons. In order to examine this, we calculated the formation rate of 1.2 nm particles (diameter of the critical cluster as suggested by Sipilä et al., 2010) with the method presented by Kerminen and Kulmala (2002) and used this $J_{1.2}$ in the model comparisons instead of J_2 (results not shown). This diminished the overall variations $V_{90/10}$ related to all of the modeled kinetic mechanisms. The variations related to K, K_{org}, K_{het}, K_{SA} and K_S decreased to values 168, 154, 24, 26 and 39, respcectively (compared to 180, 187, 32, 33 and 51 in Table 2). The variations achieved with separate kinetic nucleation coefficients for each term in Eqs. (19) and (20) also diminished, from 27 and 26 to 20 and 18, respectively. On the contrary, all the variations related to the activation-type models remained as in Table 2, or increased (variations realeated to A and A_{org}, from 12 to 13, and from 36 to 40, respectively). Additionally, the variation related to $J=B\text{GR}_{2-4}$ remained as in Table 2. The remarkable decrease of all the kinetic nucleation coefficients seems to indicate that the achieved correlations between J_2 and kinetic models involving [org] can not be explained just by the growth from the critical cluster to a particle with diameter 2 nm, but instead, that the nucleation mechanism itself is connected to those organic vapours, which affect the initial growth of the particles.

3.3.4 The different behavior of the formation rate in HPB

The closer connection of J_2 with [org] than with [H_2SO_4] in Hohenpeissenberg, while on all the other sites the [H_2SO_4] seemed to be the main determinant of J_2, can not be explained hitherto. Furthermore, Hohenpeissenberg is the only place in our knowledge where the nucleation event frequency has been observed to have maximum during the cold season instead of spring or summer (Birmili et al., 2003; Paasonen et al., 2009). It is possible that in HPB some specific low-volatility organic vapour is present in contrast to the other measurement sites, which then should be almost as active on activating the clusters or more active to nucleate homogenously than sulphuric acid. On the other hand, the different behavior might also be related to the HPB station being located on the mountain top over 300 m above the surroundings. For example Rodrigues et al. (2009) have reported different behavior of the nucleation events depending on the season at the mountain site of Teneriffe. Unfortunately, in our data there were very few analyzable nucleation events in HPB during the late spring and summer months, the time when the measurements were performed at the other sites, due to the involvement of the Hohenpeissenberg CIMS in the Melpitz and SPC campaigns. Thus, a detailed comparison of data from the same season as those of the other stations is currently not possible, but the two nucleation events recorded during spring/summer do not show correlation between nucleation rate and sulphuric acid concentration, either. Furthermore, measurements at HPB are continuously running and corresponding data should become available soon.

4 Conclusions

We evaluated the concentration of the vapours other than sulphuric acid condensing on 2 to 4 nm particles, by subtracting the calculated growth rate related to sulphuric acid condensation from the observed growth rate of these particles. We used the method

presented by Nieminen et al. (2010) to calculate the growth rate related to sulphuric acid condensation, and further to estimate the concentration of the vapours inducing the rest of the growth by assuming that these other vapours are low-volatility organic vapours, as suggested by e.g. Kulmala et al. (2004b) and Paasonen et al. (2009).

This low-volatility organic vapour concentration was used in order to find out whether and how it affects the formation rate of 2 nm sized neutral particles (J_2), determined from particle size distributions. The analysis was made for data sets collected during EUCAARI-campaigns between the years 2007 and 2009 at four European measurement sites (Hyytiälä/Finland, Hohenpeissenberg and Melpitz/Germany, and San Pietro Capofiume/Italy). The data showed a wide range of particle formation and growth rates (over three and two orders of magnitude, respectively).

We tested the models of several nucleation mechanisms, including activation- (Kulmala et al., 2006) and kinetic-type (McMurry and Friedlander, 1979) sulphuric acid nucleation mechanisms, and six additional mechanisms involving low-volatility organic vapours. These mechanisms were analogous to activation and kinetic theories, but utilizing low-volatility organic vapour concentrations alone or together with sulphuric acid concentrations instead of sulphuric acid concentrations alone. One of them, the heteromolecular homogeneous nucleation mechanism, has already been investigated in laboratory conditions by Metzger et al. (2010).

The models of the different nucleation mechanisms were compared on the basis of the following characteristics and methods: (i) the correlation coefficient R between the logarithms of the observed and modeled neutral nucleation rate, (ii) the variation $V_{90/10}$ i.e. the ratio of 90th and 10th percentiles of the data point-specific ratio between the observed and modeled formation rates, and (iii) visual analysis of the figures presenting the observed against the predicted formation rate (both in logarithmic scale), and more specifically, how close to slope one were the data points of both the whole data set and site-specific data sets in these figures. If the slope significantly differs from one, the physical reasoning behind the mechanism does not hold. For all the modeled mechanisms with more than one term (i.e. two or more mechanisms are assumed

to produce particles simultaneously), the comparison was made both with a single nucleation coefficient connecting the observed and modeled nucleation rates, and with separate nucleation coefficients for each term.

A remarkable result of our study was that at Hohenpeissenberg the nucleation rate behaved differently than at the other sites: whereas at the other sites the correlation between J_2 and sulphuric acid concentration was strong ($R > 0.55$) and that between J_2 and organic vapour concentration not ($R < 0.30$), in Hohenpeissenberg J_2 had a strong correlation with organic vapour concentration ($R = 0.61$) and a weak correlation with sulphuric acid concentration ($R = 0.17$). The different behavior of the Hohenpeissenberg data set may result from the location of the measurement site, which is on the top of the mountain (300 m above the surroundings), or from the long term nature of the measurements, as the Hohenpeissenberg data set includes nucleation events from all seasons whereas the other data were recorded during spring and summer months only. However, also the two nucleation events observed in HPB during spring/summer were in contrast to coupling between nucleation rate and sulphuric acid concentration.

The smallest variations $V_{90/10}$ for the whole data set were achieved with the models describing the cluster activation by sulphuric acid alone $J = A$ [H$_2$SO$_4$] ($V_{90/10} = 12$), and by both sulphuric acid and organic vapours with separated nucleation coefficients $J = A_{s1}$[H$_2$SO$_4$] + A_{s2}[org], where $A_{s1} = 7.3 \times 10^{-7}$ s^{-1} and $A_{s2} = 6.1 \times 10^{-8}$ s^{-1} ($V_{90/10} = 8$). Furthermore, the highest correlation coefficient related to the studied models, $R = 0.78$, was also achieved with the latter of these activation mechanisms. However, by analyzing the figures related to these models (Figs. 4 and 8), we realized that even though with these mechanisms the data points of the whole data set produced a slope very close to one, the site specific data sets were described clearly better with a steeper slope. Thus, the activation mechanisms do not describe the nucleation process reliably.

By the general inspection of the $V_{90/10}$-values achieved with the different models, we concluded that the kinetic-type mechanisms connected to second order vapour concentrations resulted in larger variations. This behavior is reasonable due to the

Full Screen / Esc

Printer-friendly Version

Interactive Discussion

propagation of error when the measured and approximated vapour concentrations are multiplied or squared. Hence, the site specific variations from the sulphuric acid kinetic nucleation theory $J=K[H_2SO_4]^2$ for the sites other than Hohenpeissenberg were relatively small ($V_{90/10}$<20), but the high variation for the whole data set ($V_{90/10}$=180) reveals that there is some clear difference affecting the nucleation at the different sites. This variation was also seen in the site-specific median values of the coefficient K, varying from 3.0×10^{-14} cm^3 s^{-1} in SPC to 1.4×10^{-12} cm^3 s^{-1} in Hyytiälä. Nevertheless, based on the visual observation, the modeled kinetic nucleation mechanisms, of organic vapours in Hohenpeissenberg and sulphuric acid at the other sites, described clearly better the site-specific data than the modeled activation mechanisms.

When taking into account all the three factors we used for estimating the representativity of the models (R, $V_{90/10}$, and the slope in figures), the most promising modeled mechanisms seemed to be the homogenous i.e. kinetic-type nucleation of sulphuric acid both homomolecularly and heteromolecularly with the low-volatility organic vapours, with or without the homomolecular nucleation of the organic vapours. By using in $J=K_{SA1}[H_2SO_4]^2+K_{SA2}[H_2SO_4][org]$ the values K_{SA1}=8.2×10^{-15} cm^3 s^{-1} and K_{SA2}=7.0×10^{-14} cm^3 s^{-1}, a good correlation for the whole data set was achieved (R=0.73, $V_{90/10}$=27). With these nucleation coefficient values, the lowest correlation coefficient for the separate sites was R=0.47 and largest variation $V_{90/10}$=31, which is reasonably low when resulting from model related to second order vapour concentrations. With this model the slope for the whole data set in figure presenting the logarithm of observed nucleation rate vs. the logarithm of modeled nucleation rate, was quite close to one. However, like all the other kinetic models, also this model predicted somewhat higher J_2 in San Pietro Capofiume than actually observed. Inserting a term of homomolecular organic vapour nucleation, i.e. $J=K_{SA1}[H_2SO_4]^2+K_{SA2}[H_2SO_4][org]+K_{SA3}[org]^2$, with the values K_{s1}=9.2×10^{-15}, K_{s2}=5.8×10^{-14} and K_{s3}=9.8×10^{-16} cm^3 s^{-1}, did not change remarkably the results (R=0.72, $V_{90/10}$=26). Achieving the best results by modeling these two mechanisms is promising, since particle formation via both the homomolecular sulphuric acid

On the roles of H$_2$SO$_4$ and organic vapours in new particle formation

P. Paasonen et al.

Title Page

Abstract | Introduction

Conclusions | References

Tables | Figures

|◄ | ►|

◄ | ►

Back | Close

Full Screen / Esc

Printer-friendly Version

Interactive Discussion

nucleation, with atmospherically relevant concentrations of H_2SO_4 (Sipilä et al., 2010), and heteromolecular nucleation between sulphuric acid and organic vapours (Metzger et al., 2010) have been recently reported in laboratory conditions.

Due to a large number of uncertainties in the measurements, the determination of the growth rates, the parameterization of the time dependence of the growth rates and the associated determination of the organic vapour concentrations, the presented values of the nucleation coefficients connecting J_2 and the vapour concentrations, are not assumed to be exact. Nevertheless, they should provide at least good order of magnitude estimates.

Our results suggest that also other condensable vapours than sulphuric acid, presumably oxidized organic vapours, do play a role in atmospheric nucleation. However, none of the modeled nucleation mechanisms resulted in indubitable closure. Furthermore, the reason for the deviant behavior of the Hohenpeissenberg data-set remained unexplained. Thus, more research on the role of condensable vapours in nucleation process, including long term measurements of sub 5 nm particle size distributions and sulphuric acid concentration, is needed.

On the roles of H$_2$SO$_4$ and organic vapours in new particle formation

P. Paasonen et al.

References

Aalto, P., Hämeri, K., Becker, E., Weber, R., Salm, J., Mäkelä, J., Hoell, C., O'Dowd, C. D., Karlson, H., Hansson, H.-C., Väkevä, M., Koponen, I. K., Buzorius, G., and Kulmala, M.: Physical characterization of aerosol particles during nucleation events, Tellus B, 53, 344–358, 2001.

Arneth, A., Monson, R. K., Schurgers, G., Niinemets, Ü., and Palmer, P. I.: Why are estimates of global terrestrial isoprene emissions so similar (and why is this not so for monoterpenes)?, Atmos. Chem. Phys., 8, 4605–4620, 2008,
http://www.atmos-chem-phys.net/8/4605/2008/.

Asmi, E., Sipilä, M., Manninen, H. E., Vanhanen, J., Lehtipalo, K., Gagné, S., Neitola, K., Mirme, A., Mirme, S., Tamm, E., Uin, J., Komsaare, K., Attoui, M., and Kulmala, M.: Results of the first air ion spectrometer calibration and intercomparison workshop, Atmos. Chem. Phys., 9, 141–154, 2009,
http://www.atmos-chem-phys.net/9/141/2009/.

Berresheim, H., Elste, T., Plass-Dülmer, C., Eisele, F. L., and Tanner, D. J.: Chemical ionization mass spectrometer for long-term measurements of atmospheric OH and H_2SO_4, Int. J. Mass Spectrom., 202, 91–109, 2000.

Birmili, W., Stratmann, F., and Wiedensohler A.: Design of a DMA-based size spectrometer for a large particle size range and stable operation, J. Aerosol Sci., 30(4), 549–553, 1999.

Birmili, W., Berresheim, H., Plass-Dülmer, C., Elste, T., Gilge, S., Wiedensohler, A., and Uhrner, U.: The Hohenpeissenberg aerosol formation experiment (HAFEX): a long-term study including size-resolved aerosol, H_2SO_4, OH, and monoterpenes measurements, Atmos. Chem. Phys., 3, 361–376, 2003,
http://www.atmos-chem-phys.net/3/361/2003/.

Boy, M., Kulmala, M., Ruuskanen, T. M., Pihlatie, M., Reissell, A., Aalto, P. P., Keronen, P., Dal Maso, M., Hellen, H., Hakola, H., Jansson, R., Hanke, M., and Arnold, F.: Sulphuric acid closure and contribution to nucleation mode particle growth, Atmos. Chem. Phys., 5, 863–878, 2005,
http://www.atmos-chem-phys.net/5/863/2005/.

Clayes, M., Iinuma, Y., Szmigielski, R., Surratt, J. D., Blockhuys, F., Van Alsenoy, C., Böge, O., Sierau, B., Gomez-Gonzalez, Y., Vermeylen, R., Van der Veken, P., Shahgholi, M., Chan, A. W. H., Herrmann, H., Seinfeld, J. H., and Maenhaut, W.: Terpenylic acid and

Title Page

Abstract | Introduction

Conclusions | References

Tables | Figures

◄ | ►

◄ | ►

Back | Close

Full Screen / Esc

Printer-friendly Version

Interactive Discussion

related compounds from the oxidation of α-pinene: Implications for new particle formation and growth above forest, Environ. Sci. Technol., 43, 6976–6982, 2009.

Engler, C., Rose, D., Wehner, B., Wiedensohler, A., Brüggemann, E., Gnauk, T., Spindler, G., Tuch, T., and Birmili, W.: Size distributions of non-volatile particle residuals ($D_p < 800$ nm) at a rural site in Germany and relation to air mass origin, Atmos. Chem. Phys., 7, 5785–5802, 2007,
http://www.atmos-chem-phys.net/7/5785/2007/.

Hallquist, M., Wenger, J. C., Baltensperger, U., Rudich, Y., Simpson, D., Claeys, M., Dommen, J., Donahue, N. M., George, C., Goldstein, A. H., Hamilton, J. F., Herrmann, H., Hoffmann, T., Iinuma, Y., Jang, M., Jenkin, M. E., Jimenez, J. L., Kiendler-Scharr, A., Maenhaut, W., McFiggans, G., Mentel, Th. F., Monod, A., Prévôt, A. S. H., Seinfeld, J. H., Surratt, J. D., Szmigielski, R., and Wildt, J.: The formation, properties and impact of secondary organic aerosol: current and emerging issues, Atmos. Chem. Phys., 9, 5155–5236, 2009,
http://www.atmos-chem-phys.net/9/5155/2009/.

Hamed, A., Joutsensaari, J., Mikkonen, S., Sogacheva, L., Dal Maso, M., Kulmala, M., Cavalli, F., Fuzzi, S., Facchini, M. C., Decesari, S., Mircea, M., Lehtinen, K. E. J., and Laaksonen, A.: Nucleation and growth of new particles in Po Valley, Italy, Atmos. Chem. Phys., 7, 355–376, 2007,
http://www.atmos-chem-phys.net/7/355/2007/.

Hamed, A., Birmili, W., Joutsensaari, J., Mikkonen, S., Asmi, A., Wehner, B., Spindler, G., Jaatinen, A., Wiedensohler, A., Korhonen, H., Lehtinen, K. E. J., and Laaksonen, A.: Changes in the production rate of secondary aerosol particles in Central Europe in view of decreasing SO_2 emissions between 1996 and 2006, Atmos. Chem. Phys., 10, 1071–1091, 2010,
http://www.atmos-chem-phys.net/10/1071/2010/.

Hao, L. Q., Yli-Pirilä, P., Tiitta, P., Romakkaniemi, S., Vaattovaara, P., Kajos, M. K., Rinne, J., Heijari, J., Kortelainen, A., Miettinen, P., Kroll, J. H., Holopainen, J. K., Smith, J. N., Joutsensaari, J., Kulmala, M., Worsnop, D. R., and Laaksonen, A.: New particle formation from the oxidation of direct emissions of pine seedlings, Atmos. Chem. Phys., 9, 8121–8137, 2009,
http://www.atmos-chem-phys.net/9/8121/2009/.

Hari, P. and Kulmala, M.: Station for measuring ecosystem-atmosphere relations (SMEAR II), Boreal Environ. Res., 10, 315–322, 2005.

On the roles of H_2SO_4 and organic vapours in new particle formation

P. Paasonen et al.

Title Page

Abstract | Introduction

Conclusions | References

Tables | Figures

◀ | ▶

◀ | ▶

Back | Close

Full Screen / Esc

Printer-friendly Version

Interactive Discussion

Hirsikko, A., Laakso, L., Horrak, U., Aalto, P. P., Kerminen, V.-M., and Kulmala, M.: Annual and size dependent variation of growth rates and ion concentrations in boreal forest, Boreal Environ. Res., 10, 357–369, 2005.

Hoppel, W. A.: Determination of the Aerosol Size Distribution from the Mobility Distribution of the Charged Fraction of Aerosols, J. Aerosol Sci., 9, 41–54, 1978.

Israël, H.: Atmospheric electricity, Israel Program for Scientific Translations, Jerusalem, Vol. 1, 1970.

Jaecker-Voirol, A.: Etude physico-chimique de la formation des aérosols: application aux "pluies acides" et la stratosphère, Thesis, Université Louis Pasteur, Dép. de Chimie, Strasbourg, France, 1988.

Jimenez, J. L., Canagaratna, M. R., Donahue, N. M., Prévôt, A. S. H., Zhang, Q., Kroll, J. H., DeCarlo, P. F., Allan, J. D., Coe, H., Ng, N. L., Aiken, A. C., Docherty, K. S., Ulbrich, I. M., Grieshop, A. P., Robinson, A. L., Duplissy, J., Smith, J. D., Wilson, K. R., Lanz, V. A., Hueglin, C., Sun, Y. L., Tian, J., Laaksonen, A., Raatikainen, T., Rautiainen, J., Vaattovaara, P., Ehn, M., Kulmala, M., Tomlinson, J. M., Collins, D. R., Cubison, M. J. E., Dunlea, J., Huffman, J. A., Onasch, T. B., Alfarra, M. R., Williams, P. I., Bower, K., Kondo, Y., Schneider, J., Drewnick, F., Borrmann, S., Weimer, S., Demerjian, K., Salcedo, D., Cottrell, L., Griffin, R., Takami, A., Miyoshi, T., Hatakeyama, S., Shimono, A., Sun, J. Y., Zhang, Y. M., Dzepina, K., Kimmel, J. R., Sueper, D., Jayne, J. T., Herndon, S. C., Trimborn, A. M., Williams, L. R., Wood, E. C., Middlebrook, A. M., Kolb, C. E., Baltensperger, U., and Worsnop, D. R.: Evolution of organic aerosols in the atmosphere, Science, 326, 1525–1529, 2009.

Kerminen, V.-M. and Kulmala, M.: Analytical formulae connecting the "real" and "apparent" nucleation rate and the nuclei number concentration for atmospheric nucleation events, J. Aerosol Sci., 33, 609–622, 2002.

Kerminen, V.-M., Lihavainen, H., Komppula, M., Viisanen, Y., and Kulmala, M.: Direct observational evidence linking atmospheric aerosol formation and cloud droplet activation, Geophys. Res. Lett., 32, L14803, doi:10.1029/2005GL023130, 2005.

Kuang, C., McMurry, P. H., McCormick, A. V., and Eisele, F. L.: Dependence of nucleation rates on sulfuric acid vapor concentration in diverse atmospheric locations, J. Geophys. Res., 113, D10209, doi:10.1029/2007JD009253, 2008.

Kulmala, M., Dal Maso, M., Mäkelä, J. M., Pirjola, L., Väkevä, M., Aalto, P. P., Miikkulainen, P., Hämeri, K., and O'Dowd, C. D.: On the formation, growth and composition of nucleation mode particles, Tellus B, 53, 479–490, 2001.

On the roles of H_2SO_4 and organic vapours in new particle formation

P. Paasonen et al.

Kulmala, M., Vehkamäki, H., Petäjä, T., Dal Maso, M., Lauri, A., Kerminen, V.-M., Birmili, W., and McMurry, P. H.: Formation and growth rates of ultrafine atmospheric particles: a review of observations, J. Aerosol Sci., 35, 146–176, 2004a.

Kulmala, M., Suni, T., Lehtinen, K. E. J., Dal Maso, M., Boy, M., Reissell, A., Rannik, Ü., Aalto, P., Keronen, P., Hakola, H., Bäck, J., Hoffmann, T., Vesala, T., and Hari, P.: A new feedback mechanism linking forests, aerosols, and climate, Atmos. Chem. Phys., 4, 557–562, 2004b, http://www.atmos-chem-phys.net/4/557/2004/.

Kulmala, M., Lehtinen, K. E. J., and Laaksonen, A.: Cluster activation theory as an explanation of the linear dependence between formation rate of 3 nm particles and sulphuric acid concentration, Atmos. Chem. Phys., 6, 787–793, 2006, http://www.atmos-chem-phys.net/6/787/2006/.

Kulmala, M., Riipinen, I., Sipilä, M., Manninen, H. E., Petäjä, T., Junninen, H., Dal Maso, M., Mordas, G., Mirme, A., Vana, M., Hirsikko, A., Laakso, L., Harrison, R. M., Hanson, I., Leung, C., Lehtinen, K. E. J., and Kerminen, V.-M.: Toward direct measurement of atmospheric nucleation, Science, 318, 89–92, 2007.

Kulmala, M. and Kerminen, V.-M.: On the growth of atmospheric nanoparticles, Atmos. Res., 90, 132–150, 2008.

Kulmala, M., Asmi, A., Lappalainen, H. K., Carslaw, K. S., Pöschl, U., Baltensperger, U., Hov, Ø., Brenquier, J.-L., Pandis, S. N., Facchini, M. C., Hansson, H.-C., Wiedensohler, A., and O'Dowd, C. D.: Introduction: European Integrated Project on Aerosol Cloud Climate and Air Quality interactions (EUCAARI) - integrating aerosol research from nano to global scales, Atmos. Chem. Phys., 9, 2825–2841, 2009, http://www.atmos-chem-phys.net/9/2825/2009/.

Kurtén, T., Noppel, M., Vehkamäki, H., Salonen, M., and Kulmala, M.: Quantum chemical studies of hydrate formation of H_2SO_4 and HSO_4, Boreal Environ. Res., 12, 431–453, 2007.

Laaksonen, A., Hamed, A., Joutsensaari, J., Hiltunen, L., Cavalli, F., Junkermann, W., Asmi, A., Fuzzi, S., and Facchini, M. C.: Cloud condensation nuclei production from nucleation events at a highly polluted region, Geophys. Res. Lett., 32, L06812, doi:10.1029/2004GL022092, 2005.

Laaksonen, A., Kulmala, M., O'Dowd, C. D., Joutsensaari, J., Vaattovaara, P., Mikkonen, S., Lehtinen, K. E. J., Sogacheva, L., Dal Maso, M., Aalto, P., Petäjä, T., Sogachev, A., Yoon, Y. J., Lihavainen, H., Nilsson, D., Facchini, M. C., Cavalli, F., Fuzzi, S., Hoffmann, T., Arnold, F., Hanke, M., Sellegri, K., Umann, B., Junkermann, W., Coe, H., Allan, J. D., Alfarra, M. R.,

On the roles of H_2SO_4 and organic vapours in new particle formation

P. Paasonen et al.

Title Page

Abstract | Introduction

Conclusions | References

Tables | Figures

|◄ | ►|

◄ | ►

Back | Close

Full Screen / Esc

Printer-friendly Version

Interactive Discussion

Worsnop, D. R., Riekkola, M. -L., Hyötyläinen, T., and Viisanen, Y.: The role of VOC oxidation products in continental new particle formation, Atmos. Chem. Phys., 8, 2657–2665, 2008, http://www.atmos-chem-phys.net/8/2657/2008/.

Lehtinen, K. E. J. and Kulmala, M.: A model for particle formation and growth in the atmosphere with molecular resolution in size, Atmos. Chem. Phys., 3, 251–257, 2003, http://www.atmos-chem-phys.net/3/251/2003/.

Lihavainen, H., Kerminen, V.-M., Komppula, M., Hatakka, J., Aaltonen, V., Kulmala, M., and Viisanen, Y.: Production of "potential" cloud condensation nuclei associated with atmospheric new-particle formation in northern Finland, J. Geophys. Res., 108(D24), 4782, doi:10.1029/2003JD003887, 2003.

Makkonen, R., Asmi, A., Korhonen, H., Kokkola, H., Järvenoja, S., Räisänen, P., Lehtinen, K. E. J., Laaksonen, A., Kerminen, V.-M., Järvinen, H., Lohmann, U., Bennartz, R., Feichter, J., and Kulmala, M.: Sensitivity of aerosol concentrations and cloud properties to nucleation and secondary organic distribution in ECHAM5-HAM global circulation model, Atmos. Chem. Phys., 9, 1747–1766, 2009, http://www.atmos-chem-phys.net/9/1747/2009/.

Manninen, H. E., Nieminen, T., Riipinen, I., Yli-Juuti, T., Gagné, S., Asmi, E., Aalto, P. P., Petäjä, T., Kerminen, V.-M., and Kulmala, M.: Charged and total particle formation and growth rates during EUCAARI 2007 campaign in Hyytiälä, Atmos. Chem. Phys., 9, 4077–4089, 2009, http://www.atmos-chem-phys.net/9/4077/2009/.

Manninen, H. E., Nieminen, T., Asmi, E., Gagné, S., Häkkinen, S., Lehtipalo, K., Aalto, P., Vana, M., Mirme, A., Mirme, S., Hõrrak, U., Plass-Dülmer, C., Stange, G., Kiss, G., Hoffer, A., Törő, N., Moerman, M., Henzing, B., de Leeuw, G., Brinkenberg, M., Kouvarakis, G. N., Bougiatioti, A., Mihalopoulos, N., O'Dowd, C., Ceburnis, D., Arneth, A., Svenningsson, B., Swietlicki, E., Tarozzi, L., Decesari, S., Facchini, M. C., Birmili, W., Sonntag, A., Wiedensohler, A., Boulon, J., Sellegri, K., Laj, P., Gysel, M., Bukowiecki, N., Weingartner, E., Wehrle, G., Laaksonen, A., Hamed, A., Joutsensaari, J., Petäjä, T., Kerminen, V.-M., and Kulmala, M.: EUCAARI ion spectrometer measurements at 12 European sites - analysis of new-particle formation events, Atmos. Chem. Phys. Discuss., 10, 11251–11313, 2010, http://www.atmos-chem-phys-discuss.net/10/11251/2010/.

McMurry, P. H. and Friedlander, S. K.: New particle formation in the presence of aerosol, Atmos. Environ., 13, 1635–1651, 1979.

On the roles of H_2SO_4 and organic vapours in new particle formation

P. Paasonen et al.

Title Page

Abstract	Introduction
Conclusions	References
Tables	Figures

|◄ | ►|

◄ | ►

Back | Close

Full Screen / Esc

Printer-friendly Version

Interactive Discussion

Merikanto, J., Spracklen, D. V., Mann, G. W., Pickering, S. J., and Carslaw, K. S.: Impact of nucleation on global CCN, Atmos. Chem. Phys., 9, 8601–8616, 2009, http://www.atmos-chem-phys.net/9/8601/2009/.

Metzger, A., Verheggen, B., Dommen, J., Duplissy, J., Prevot, A. S., Weingartner, E., Riipinen, I., Kulmala, M., Spracklen, D. V., Carslaw, K. S., and Baltensperger, U.: Evidence for the role of organics in aerosol particle formation under atmospheric conditions, P. Natl. Acad. Sci., 107, 6646–6651, doi:10.1073/pnas.0911330107, 2010.

Mirme, S., Mirme, A., Minikin, A., Petzold, A., Hõrrak, U., Kerminen, V. -M., and Kulmala, M.: Atmospheric sub-3 nm particles at high altitudes, Atmos. Chem. Phys., 10, 437–451, 2010, http://www.atmos-chem-phys.net/10/437/2010/.

Nieminen, T., Manninen, H. E., Sihto, S.-L., Yli-Juuti, T., Mauldin III, R. L., Petäjä, T., Riipinen, I., Kerminen, V.-M., and Kulmala, M.: Connection of sulfuric acid to atmospheric nucleation in boreal forest, Environ. Sci. Technol., 43, 4715–4721, 2009.

Nieminen, T., Lehtinen, K. E. J., and Kulmala, M.: On condensational growth of clusters and nanoparticles in sub-10 nm size range, Atmos. Chem. Phys. Discuss., 10, 1693–1717, 2010, http://www.atmos-chem-phys-discuss.net/10/1693/2010/.

O'Dowd, C. D., Aalto, P. P., Hämeri, K., and Kulmala, M.: Atmospheric particles from organic vapours, Nature, 416, 497–498, 2002.

Paasonen, P., Sihto, S.-L., Nieminen, T., Vuollekoski, H., Riipinen, I., Plass-Dülmer, C., Berresheim, H., Birmili, W., and Kulmala, M.: Connection between new particle formation and sulphuric acid at Hohenpeissenberg (Germany) including the influence of organic compounds, Boreal Environ. Res., 14, 616–629, 2009.

Pacifico, F., Harrison, S. P., Jones, C. D., and Sitch, S.: Isoprene emissions and climate, Atmos. Environ., 43, 6121–6135, 2009.

Petäjä, T., Mauldin, III, R. L., Kosciuch, E., McGrath, J., Nieminen, T., Paasonen, P., Boy, M., Adamov, A., Kotiaho, T., and Kulmala, M.: Sulfuric acid and OH concentrations in a boreal forest site, Atmos. Chem. Phys., 9, 7435–7448, 2009, http://www.atmos-chem-phys.net/9/7435/2009/.

Pierce, J. R. and Adams, P. J.: Uncertainty in global CCN concentrations from uncertain aerosol nucleation and primary emission rates, Atmos. Chem. Phys., 9, 1339–1356, 2009, http://www.atmos-chem-phys.net/9/1339/2009/.

Title Page

Abstract | Introduction

Conclusions | References

Tables | Figures

|◄ | ►|

◄ | ►

Back | Close

Full Screen / Esc

Printer-friendly Version

Interactive Discussion

Riipinen, I., Sihto, S.-L., Kulmala, M., Arnold, F., Dal Maso, M., Birmili, W., Saarnio, K., Teinilä, K., Kerminen, V.-M., Laaksonen, A., and Lehtinen, K. E. J.: Connections between atmospheric sulphuric acid and new particle formation during QUEST IIIIV campaigns in Heidelberg and Hyytiälä, Atmos. Chem. Phys., 7, 1899–1914, 2007,
5   http://www.atmos-chem-phys.net/7/1899/2007/.
Riipinen, I., Manninen, H. E., Yli-Juuti, T., Boy, M., Sipilä, M., Ehn, M., Junninen, H., Petäjä, T., and Kulmala, M.: Applying the Condensation Particle Counter Battery (CPCB) to study the water-affinity of freshly-formed 2-9 nm particles in boreal forest, Atmos. Chem. Phys., 9, 3317–3330, 2009,
10   http://www.atmos-chem-phys.net/9/3317/2009/.
Rinne, J., Bäck, J., and Hakola, H.: Biogenic volatile organic compound emissions from the Eurasian taiga: current knowledge and future directions, Boreal Environ. Res., 14, 807–826, 2009.
Rodríguez, S., González, Y., Cuevas, E., Ramos, R., Romero, P. M., Abreu-Afonso, J., and
15   Redondas, A.: Atmospheric nanoparticle observations in the low free troposphere during upward orographic flows at Izaa Mountain Observatory, Atmos. Chem. Phys., 9, 6319–6335, 2009,
       http://www.atmos-chem-phys.net/9/6319/2009/.
Rohrer, F. and Berresheim, H.: Strong correlation between levels of tropospheric hydroxyl radi-
20   cals and solar ultraviolet radiation, Nature, 442, 184-187, 2006.
Sihto, S.-L., Kulmala, M., Kerminen, V.-M., Dal Maso, M., Petäjä, T., Riipinen, I., Korhonen, H., Arnold, F., Janson, R., Boy, M., Laaksonen, A., and Lehtinen, K. E. J.: Atmospheric sulphuric acid and aerosol formation: implications from atmospheric measurements for nucleation and early growth mechanisms, Atmos. Chem. Phys., 6, 4079–4091, 2006,
25   http://www.atmos-chem-phys.net/6/4079/2006/.
Sipilä, M., Berndt, T., Petäjä, T., Brus, D., Vanhanen, J., Stratmann, F., Patokoski, J., Mauldin III, R. L., Hyvärinen, A.-P., Lihavainen, H., and Kulmala, M.: The role of sulphuric acid in atmospheric nucleation, Science, 327, 1243–1246, 2010.
Smith, J. N., Dunn, M. J., Van Reken, T. M., Iida, K., Stolzenburg, M. R., McMurry, P. H., and
30   Huey, L. G.: Chemical composition of atmospheric nanoparticles formed from nucleation in Tecamac, Mexico: Evidence for an important role for organic species in nanoparticle growth, Geophys. Res. Lett., 35, L04808, doi:10.1029/2007GL032523, 2008.

Title Page

Abstract | Introduction

Conclusions | References

Tables | Figures

◄ | ►|

◄ | ►

Back | Close

Full Screen / Esc

Printer-friendly Version

Interactive Discussion

Spracklen, D. V., Carslaw, K. S., Kulmala, M., Kerminen, V.-M., Sihto, S.-L., Riipinen, I., Merikanto, J., Mann, G. W., Chipperfield, M. P., Wiedensohler, A., Birmili, W., and Lihavainen, H.: Contribution of particle formation to global cloud condensation nuclei concentrations, Geophys. Res. Lett., 35, L06808, doi:10.1029/2007GL033038, 2008.

Taipale, R., Ruuskanen, T. M., Rinne, J., Kajos, M. K., Hakola, H., Pohja, T., and Kulmala, M.: Technical Note: Quantitative long-term measurements of VOC concentrations by PTR-MS - measurement, calibration, and volume mixing ratio calculation methods, Atmos. Chem. Phys., 8, 6681–6698, 2008,
http://www.atmos-chem-phys.net/8/6681/2008/.

Tammet, H. and Kulmala, M.: Simulation tool for atmospheric aerosol nucleation bursts, J. Aerosol Sci., 36, 173–196, 2005.

Venzac, H., Sellegri, K., Laj, P., Villani, P., Bonasoni, P., Marinoni, A., Cristofanelli, P., Calzolari, F., Fuzzi, S., Decesari, S., Facchini, M. C., Vuillermoz, E., and Verza, G. P.: High Frequency New Particle Formation in the Himalayas, P. Natl. Acad. Sci., 105, 15666–15671, 2008.

Whitehead, J. D., McFiggans, G. B., Gallagher, M. W., and Flynn, M. J.: Direct linkage between tidally driven coastal ozone deposition fluxes, particle emission fluxes, and subsequent CCN formation, Geophys. Res. Lett., 36, L04806, doi:10.1029/2008GL035969, 2009.

Wiedensohler, A., Cheng, Y. F., Nowak, A., Wehner, B., Achtert, P., Berghof, M., Birmili, W., Wu, Z. J., Hu, M., Zhu, T., Takegawa, N., Kita, K., Kondo, Y., Lou, S. R., Hofzumahaus, A., Holland, F., Wahner, A., Gunthe, S. S., Rose, D., Su, H., and Pöschl, U.: Rapid aerosol particle growth and increase of cloud condensation nucleus activity by secondary aerosol formation and condensation: A case study for regional air pollution in northeastern China, J. Geophys. Res., 114, D00G08, doi:10.1029/2008JD0101884, 2009.

Wang, M. and Penner, J. E.: Aerosol indirect forcing in a global model with particle nucleation, Atmos. Chem. Phys., 9, 239–260, 2009,
http://www.atmos-chem-phys.net/9/239/2009/.

Weber, R. J., Marti, J. J., McMurry, P. H., Eisele, F. L., Tanner, D. J., and Jefferson, A.: Measurements of new particle formation and ultrafine particle growth rates at a clean continental site, J. Geophys. Res., 102, 4375–4385, 1997.

York, D., Evensen, N. M., López Martinez, M., and De Basabe Delgado, J.: Unified equations for the slope, intercept, and standard errors of the best straight line, Am. J. Phys., 72(3), 367–375, 2004.

Title Page

Abstract | Introduction

Conclusions | References

Tables | Figures

◄ | ►I

◄ | ►

Back | Close

Full Screen / Esc

Printer-friendly Version

Interactive Discussion

Yu, F. and Luo, G.: Simulation of particle size distribution with a global aerosol model: contribution of nucleation to aerosol and CCN number concentrations, Atmos. Chem. Phys., 9, 7691–7710, 2009,
http://www.atmos-chem-phys.net/9/7691/2009/.

Zhang, R., Suh, I., Zhao, J., Zhang, D., Fortner, E. C., Tie, X., Molina, L. T., and Molina, M. J.: Atmospheric New particle formation enhanced by organic acids, Science, 304, 1487–1490, 2004.

Zhang, R., Wang, L., Khalizov, A. F., Zhao, J., Zheng, J., McGraw, R. L., and Molina, L. T.: Formation of nanoparticles of blue haze enhanced by anthropogenic pollution, P. Natl. Acad. Sci., 106, 17650–17654, 2009.

On the roles of H$_2$SO$_4$ and organic vapours in new particle formation

P. Paasonen et al.

Table 1. Statistics of the new particle formation events at different measurement sites. The observed growth rates GR$_{det}$ are median values for all the events. The tabulated median values for sulphuric acid concentration [H$_2$SO$_4$], low-volatility organic vapour concentration [org], neutral particle formation rate J_2 and ion formation rate J_2^{ion} as a sum of J_2^+ and J_2^- are calculated from the data points measured during the nucleation events.

	Analyzed events, #	Data from months	GR$_{det}$, (nm/h)	[H$_2$SO$_4$], (10^6 cm^{-3})	[org], (10^6 cm^{-3})	J_2, (cm^{-3} s^{-1})	J_2^{ion}, (cm^{-3} s^{-1})
Hyytiälä	10	April–May	3.3	1.1	11	1.9	0.041
HPB	15	Full year	4.8	2.3	33	2.3	0.094
Melpitz	8	May	4.2	18	11	9.4	0.036
SPC	3	(June–)July	9.5	19	36	13	0.17

Table 2. Correlation coefficients R and variations $V_{90/10}$ achieved with all the tested nucleation mechanism models.

Nucleation mechanism		Correlation coefficient R					Variation $V_{90/10}$				
Measurement site (number of data points)		All (860)	HYY (295)	HPB (287)	MEL (202)	SPC (76)	All (860)	HYY (295)	HPB (287)	MEL (202)	SPC (76)
$J_2 = A[H_2SO_4]$	(Eq. 10)	0.66	0.58	0.17	0.69	0.59	12	9	22	7	5
$J_2 = K[H_2SO_4]^2$	(11)	0.66	0.58	0.17	0.69	0.59	180	18	99	11	8
$J_2 = A_{org}[org]$	(12)	0.18	0.29	0.61	−0.21	0.09	36	23	8	33	11
$J_2 = K_{org}[org]^2$	(13)	0.18	0.29	0.61	−0.21	0.09	187	174	17	135	15
$J_2 = A_s([H_2SO_4]+[org])$	(14)	0.52	0.36	0.61	0.55	0.35	17	17	9	9	8
$J_2 = K_{het}[H_2SO_4][org]$	(15)	0.61	0.51	0.47	0.30	0.47	32	22	30	11	9
$J_2 = K_{SA}([H_2SO_4]^2+[H_2SO_4][org])$	(16)	0.68	0.54	0.45	0.68	0.54	33	16	34	8	8
$J_2 = K_s([H_2SO_4]^2+[H_2SO_4][org]+[org]^2)$	(17)	0.53	0.33	0.61	0.66	0.35	51	120	16	8	11
$J_2 = A_{s1}[H_2SO_4]+A_{s2}[org]$	(18)	0.78	0.56	0.50	0.69	0.58	8	8	11	7	6
$J_2 = K_{SA1}[H_2SO_4]^2+K_{SA2}[H_2SO_4][org]$	(19)	0.73	0.58	0.47	0.49	0.48	27	21	31	8	8
$J_2 = K_{s1}[H_2SO_4]^2+K_{s2}[H_2SO_4][org]+K_{s3}[org]^2$	(20)	0.72	0.40	0.52	0.52	0.48	26	27	23	8	8
$J_2 = B\,GR_{2-4}$		0.49	0.35	0.61	0.50	0.32	18	18	9	10	8

Table 3. Values of the optimized separate nucleation coefficients, with the corresponding correlation coefficients R and variations $V_{90/10}$.

Nucleation mechanism		K_{s1} or K_{SA1} (10^{-14} cm^3 s^{-1})	K_{s2} or K_{SA2} (10^{-14} cm^3 s^{-1})	K_{s3} (10^{-14} cm^3 s^{-1})	A_{s1} (10^{-7} s^{-1})	A_{s2} (10^{-7} s^{-1})	R	$V_{90/10}$
$J_2 = A_{s1}[H_2SO_4] + A_{s2}[org]$	(Eq. 18)	–	–	–	7.3	0.61	0.78	8
$J_2 = K_{SA1}[H_2SO_4]^2 + K_{SA2}[H2SO4][org]$	(19)	0.82	7.0	–	–	–	0.73	27
$J_2 = K_{s1}[H_2SO_4]^2 + K_{s2}[H_2SO_4][org] + K_{s3}[org]^2$	(20)	0.92	5.8	0.098	–	–	0.72	26

Table 4. Mean, median and percentile (10th, 25th, 75th and 90th) values of the nucleation coefficients for the whole data set, and median values for separate measurement sites. The mean, median and percentile values of the ratios between the observed and modeled nucleation rates are presented related to the mechanisms including separate nucleation coefficients (the values of which are presented in Table 3).

Nucleation coefficient		Mean	Median	Percentiles				Site specific medians			
				10th	25th	75th	90th	HYY	HPB	MEL	SPC
$A(10^{-7}\,\mathrm{s}^{-1})$	(Eq. 10)	17	9.7	2.6	4.6	19	32	19	8.6	6.0	6.5
$K(10^{-14}\,\mathrm{cm}^3\,\mathrm{s}^{-1})$	(11)	140	26	2.0	5.2	140	350	140	33	3.4	3.0
$A_{\mathrm{org}}(10^{-7}\,\mathrm{s}^{-1})$	(12)	9.0	1.9	0.37	0.74	5.4	14	1.9	0.76	8.7	3.5
$K_{\mathrm{org}}(10^{-14}\,\mathrm{cm}^3\,\mathrm{s}^{-1})$	(13)	31	1.0	0.11	0.25	4.7	21	1.6	0.24	8.5	1.0
$A_{\mathrm{S}}(10^{-7}\,\mathrm{s}^{-1})$	(14)	2.6	1.5	0.34	0.66	3.3	5.8	1.6	0.67	3.5	2.3
$K_{\mathrm{het}}(10^{-14}\,\mathrm{cm}^3\,\mathrm{s}^{-1})$	(15)	16	5.6	1.0	2.3	15	34	16	3.0	6.0	1.8
$K_{\mathrm{SA}}(10^{-14}\,\mathrm{cm}^3\,\mathrm{s}^{-1})$	(16)	11	3.4	0.72	1.5	12	24	14	2.6	1.9	1.1
$K_{\mathrm{S}}(10^{-14}\,\mathrm{cm}^3\,\mathrm{s}^{-1})$	(17)	2.5	0.69	0.10	0.22	1.8	5.2	1.4	0.21	1.5	0.53
$\dfrac{J_2}{A_{\mathrm{S1}}[\mathrm{H_2SO_4}]+A_{\mathrm{S2}}[\mathrm{org}]}$	(18)	1.2	1.0	0.30	0.54	1.6	2.4	1.2	0.57	0.76	0.78
$\dfrac{J_2}{K_{\mathrm{SA1}}[\mathrm{H_2SO_4}]^2+K_{\mathrm{SA2}}[\mathrm{H_2SO_4}][\mathrm{org}]}$	(19)	2.4	1.0	0.19	0.40	2.5	5.1	2.3	0.42	0.66	0.23
$\dfrac{J_2}{K_{\mathrm{SA1}}[\mathrm{H_2SO_4}]^2+K_{\mathrm{SA2}}[\mathrm{H_2SO_4}][\mathrm{org}]+K_{\mathrm{SA3}}[\mathrm{org}]^2}$	(20)	2.6	1.0	0.21	0.43	2.5	5.6	2.3	0.38	0.74	0.27

Title Page

Abstract | Introduction

Conclusions | References

Tables | Figures

◀ | ▶

◀ | ▶

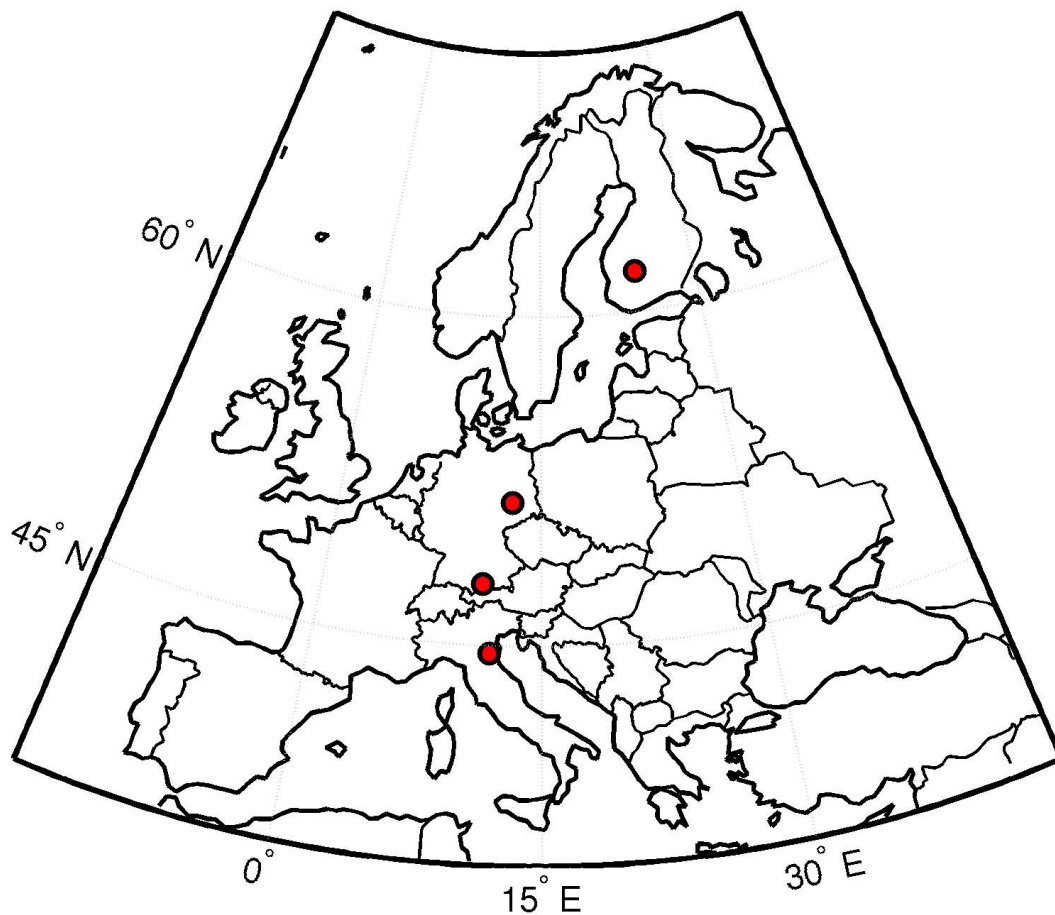Back | Close

Full Screen / Esc

Fig. 1. Map of the measurement sites. Sites from north to south: Hyytiälä (Finland), Melpitz (Germany), Hohenpeissenberg (Germany) and San Pietro Capofiume (Italy).

Title Page

Abstract | Introduction

Conclusions | References

Tables | Figures

◄ | ►

◄ | ►

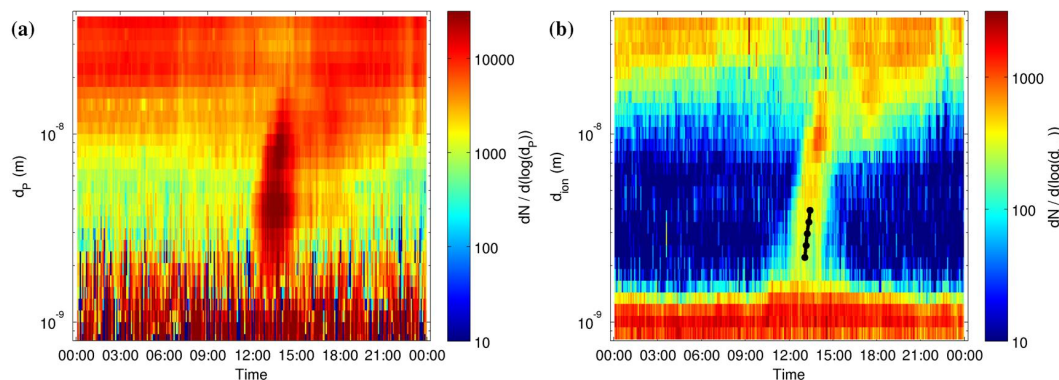Back | Close

Full Screen / Esc

Printer-friendly Version

Interactive Discussion

Fig. 2. Nucleation event recorded with the NAIS in Hohenpeissenberg on 21 September 2008. Panel **(a)** presents the total particle size distribution as a function of time. Corresponding particle concentrations are shown with colors. From this day, the data points measured between 11:30 and 14:50 were used in the analysis. Panel **(b)** shows the simultaneously measured size distributions of negative air ions. Growth rates at different size ranges are determined based on fitted modes, the maxima of which are marked with black circles. Note the different concentration scales in panels (a) and (b).
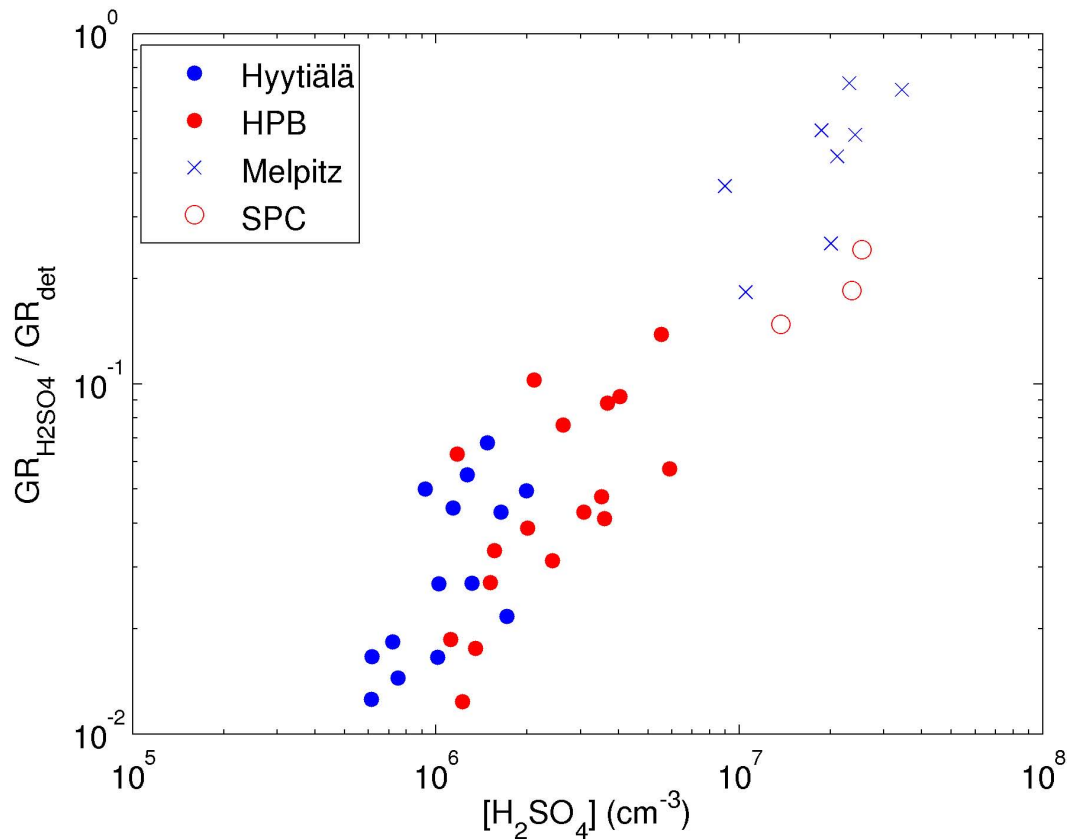
Fig. 3. The ratio between calculated growth rate due to sulphuric acid condensation and the growth rate determined from particle size distributions, as a function of sulphuric acid concentration at four measurement sites.

Title Page

Abstract | Introduction

Conclusions | References

Tables | Figures

◄◄ | ►►

◄ | ►

Back | Close

Full Screen / Esc

Printer-friendly Version

Interactive Discussion
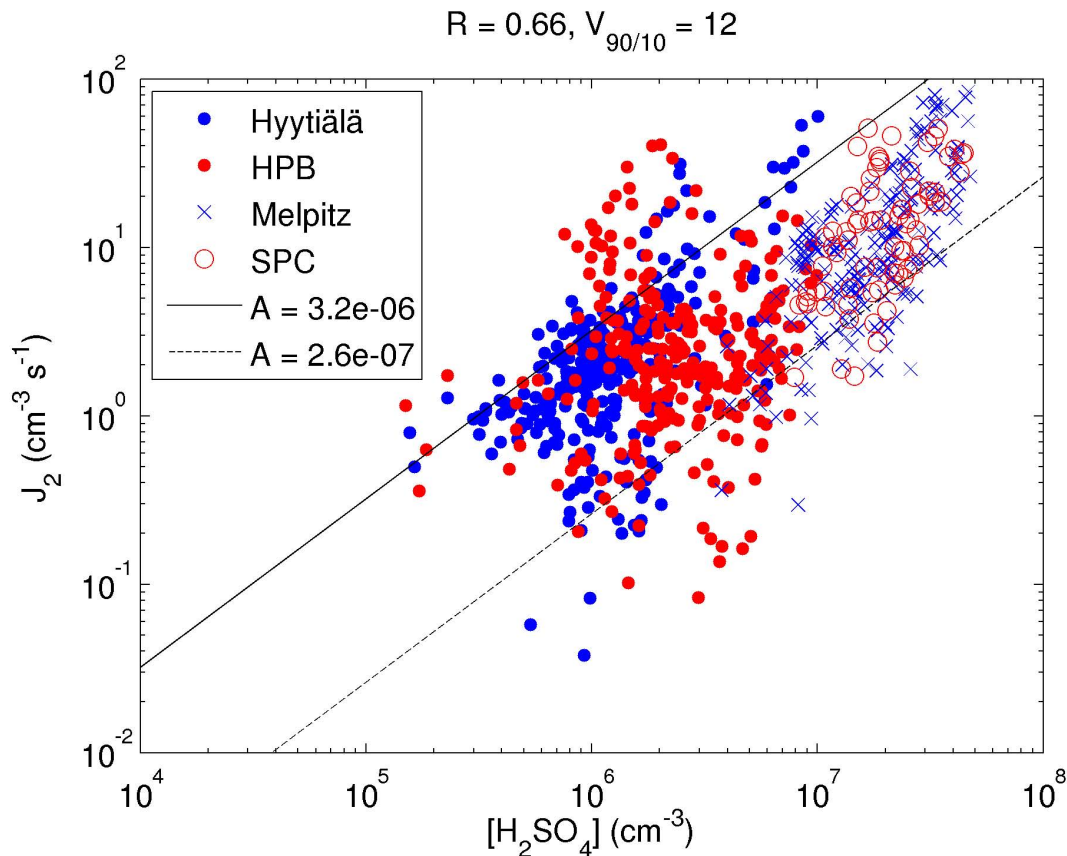
Fig. 4. Neutral particle formation rate J_2 as a function of sulphuric acid concentration. The lines present the 90th and 10th percentile values of the activation coefficient A (Eq. 10), the values of which are given in units (s^{-1}).
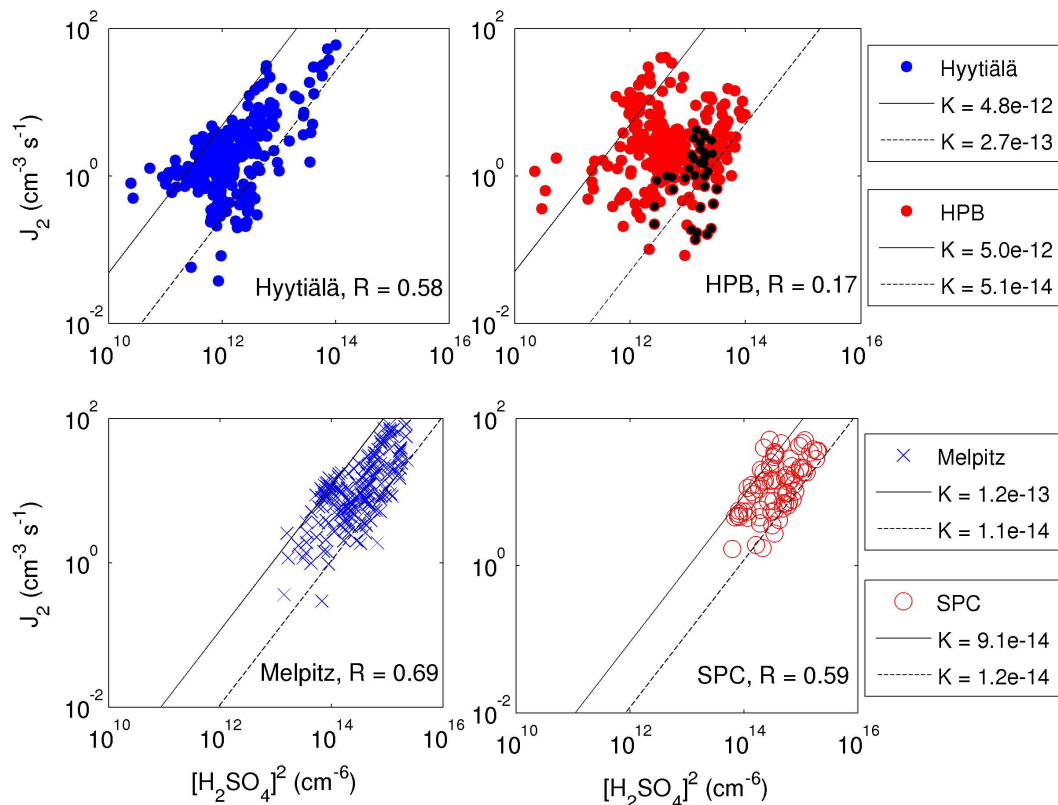
Fig. 5. Neutral particle formation rate J_2 as a function of squared sulphuric acid concentration separately for each measurement site. In the Hohenpeissenberg plot (upper right) the black points indicate the data recorded between April and July, whereas at the other sites all the data are from these months. The lines present the site-specific 90th and 10th percentile values of the kinetic coefficient K (Eq. 11), the values of which are presented in units ($cm^3 s^{-1}$) on the right hand side.
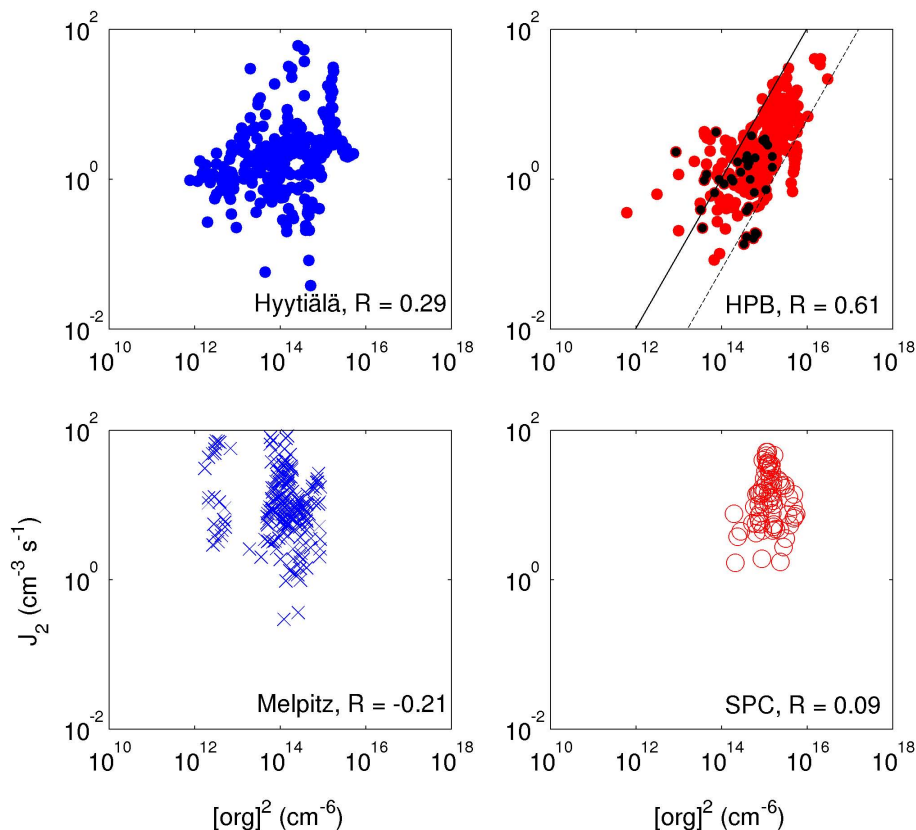
Fig. 6. Neutral particle formation rate J_2 as a function of low-volatility organic vapour concentration separately at the measurement sites. In the Hohenpeissenberg plot (upper right) the black points indicate the data recorded between April and July, whereas at the other sites all the data are from these months. The lines in Hohenpeissenberg plot present the site-specific 90th and 10th percentile values of the coefficient K_{org} (Eq. 13), 9.8×10^{-15} and 5.9×10^{-16} cm^3 s^{-1}, respectively.

Title Page

Abstract | Introduction

Conclusions | References

Tables | Figures

◄ | ►►

◄ | ►

Back | Close

Full Screen / Esc

Printer-friendly Version
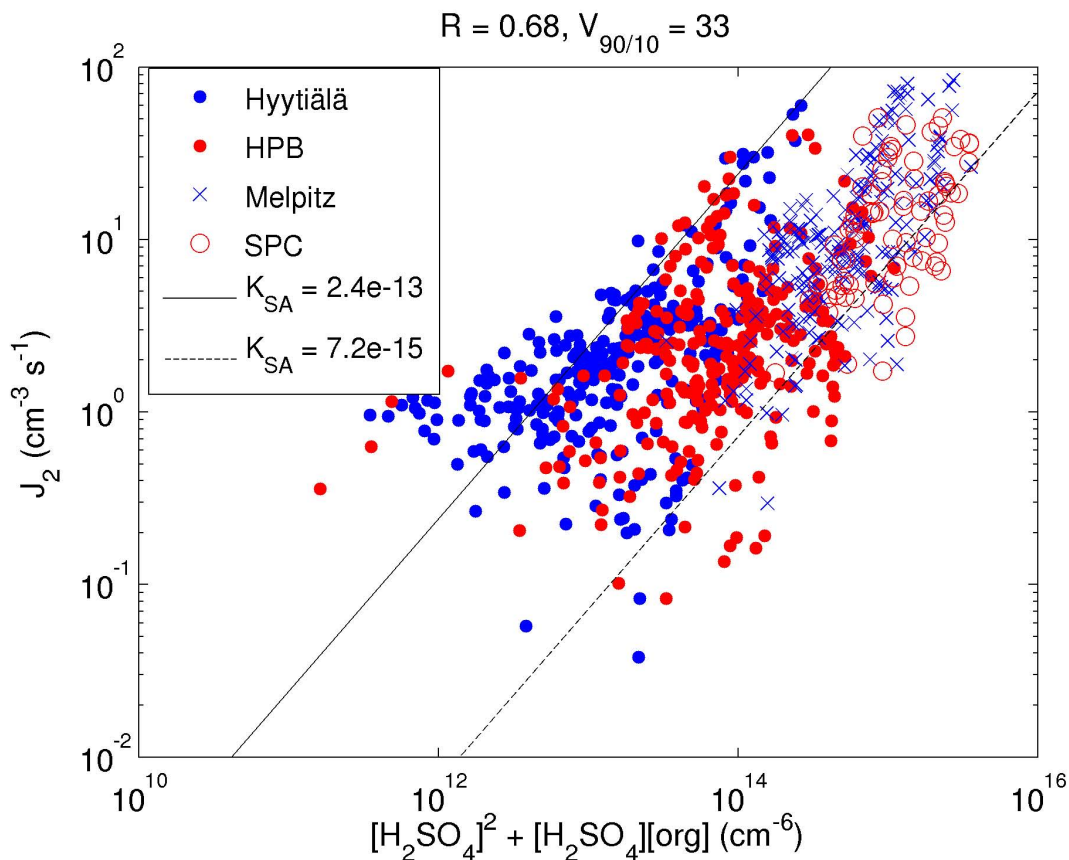
Interactive Discussion

Fig. 7. Neutral particle formation rate J_2 as a function of sum of the squared sulphuric acid concentration and the product of sulphuric acid and organic vapour concentrations. The lines present the 90th and 10th percentile values of the coefficient K_{SA} (Eq. 16), the values of which are presented in units ($cm^3 s^{-1}$).

Title Page

Abstract | Introduction

Conclusions | References

Tables | Figures

◄◄ | ►►

◄ | ►

Back | Close

Full Screen / Esc

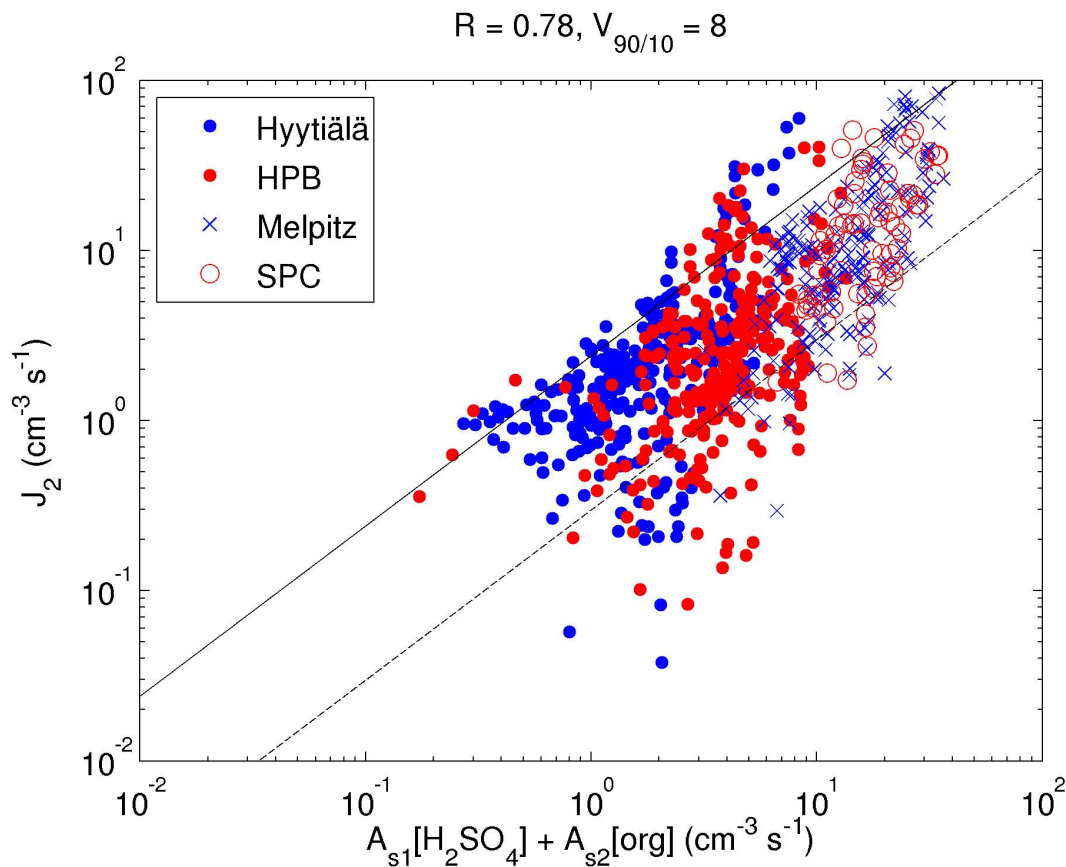Printer-friendly Version

Interactive Discussion

Fig. 8. Neutral particle formation rate J_2 as a function of the sum of sulphuric acid and low-volatility organic vapour concentrations multiplied with separate nucleation coefficients $A_{s1}=5.8\times10^{-7}$ and $A_{s2}=5.4\times10^{-8}$ s^{-1}. The lines present the 90th (solid) and 10th (dashed) percentile values of the ratio between the observed J_2 and the rate modeled with Eq. (18).
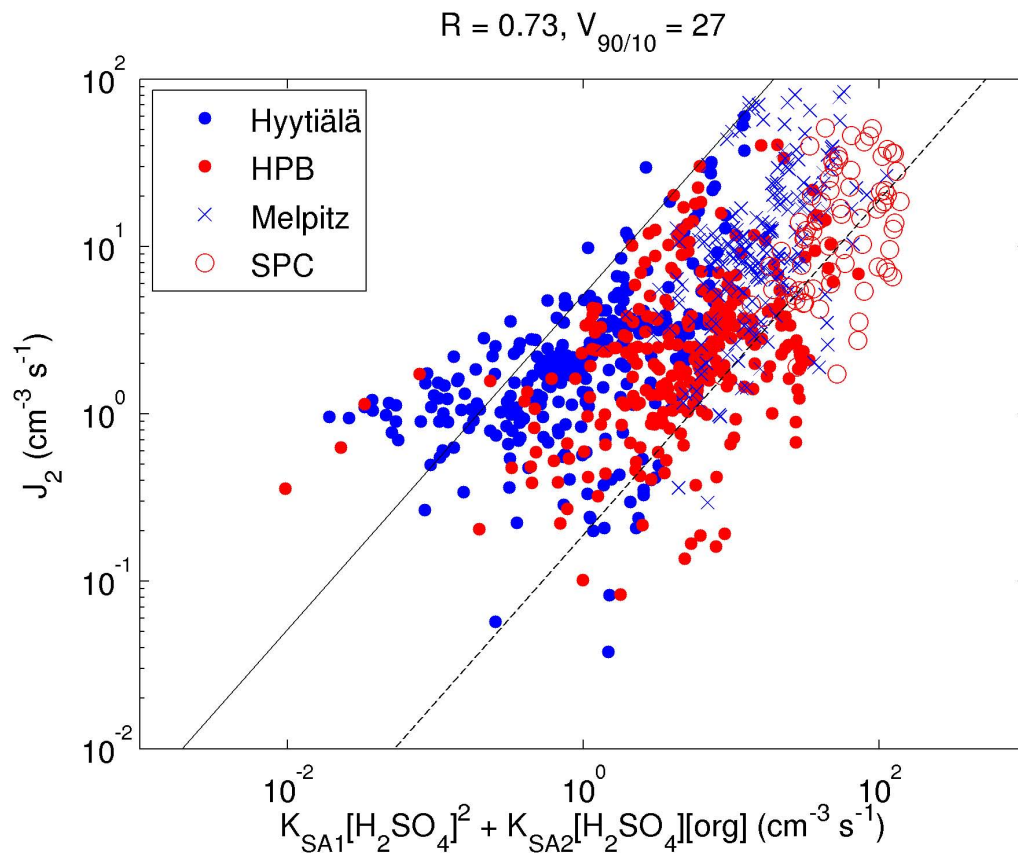
Fig. 9. Neutral particle formation rate J_2 as a function of sum of the squared sulphuric acid concentration and the product of sulphuric acid and organic vapour concentrations, terms multiplied with separate nucleation coefficients $K_{SA1}=9.5\times10^{-15}$ and $K_{SA2}=4.6\times10^{-14}$ cm^3 s^{-1}. The lines present the 90th and 10th percentile values of the ratio between the observed J_2 and the rate modeled with Eq. (19).